

Bayesian Inference of Reproduction Number from Epidemiological and Genetic Data Using Particle MCMC

Alicia Gill*[†], Jere Koskela[‡], Xavier Didelot*[§], Richard G. Everitt*

November 2019

Abstract

Inference of the reproduction number through time is of vital importance during an epidemic outbreak. Typically, epidemiologists tackle this using observed prevalence or incidence data. However, prevalence and incidence data alone is often noisy or partial. Models can also have identifiability issues with determining whether a large amount of a small epidemic or a small amount of a large epidemic has been observed. Sequencing data however is becoming more abundant, so approaches which can incorporate genetic data are an active area of research. We propose using particle MCMC methods to infer the time-varying reproduction number from a combination of prevalence data reported at a set of discrete times and a dated phylogeny reconstructed from sequences. We validate our approach on simulated epidemics with a variety of scenarios. We then apply the method to a real data set of HIV-1 in North Carolina, USA, between 1957 and 2019.

1 Introduction

The basic reproduction number, denoted R_0 , is a measure of the inherent transmissibility of a disease. It is defined as the average number of new infections caused by a single infected individual when entering a completely susceptible population (Lash et al. 2021). However, for most diseases, as the disease spreads through the population, the number of susceptibles decreases. The (effective) reproduction number, denoted R_t , represents the average number of new infections caused by a single infected individual at time t . When $R_t < 1$, the epidemic is shrinking and when $R_t > 1$, the epidemic is growing. The aim of infectious disease control programmes is to push R_t below 1. As such, estimation of the reproduction number R_t is of vital importance during an epidemic outbreak to decide which control measures to implement and to determine their effects once implemented.

Epidemiologists typically infer reproduction number R_t using prevalence and/or incidence data (Wallinga and Teunis 2004, Cori et al. 2013, Boonpatcharanon et al. 2022). However, data relating to cases is often noisy, partially observed and biased. It can also be difficult to identify whether you have observed many cases of a small epidemic or few cases of a large epidemic. In fact, modelling approaches to find the reporting probability of an epidemic is an active area of research (Gamado et al. 2014, Gamado et al. 2017, Stoner et al. 2019, Liang et al. 2022). Given these challenges with epidemiological data, genetic data, typically in the form of a dated phylogeny (see Section 1.1), is increasingly being used to understand infectious disease epidemiology (Rasmussen et al. 2011, Vaughan et al. 2019).

*Department of Statistics, University of Warwick, UK

[†]Corresponding author. Email: alicia.gill@warwick.ac.uk

[‡]School of Mathematics, Statistics and Physics, Newcastle University, UK

[§]School of Life Sciences, University of Warwick, UK

To combine partial epidemiological information together with the genetic data, we take a Bayesian approach to find the posterior distribution of R_t given the partially observed epidemic and the genetic data. We then use pseudo-marginal MCMC (Andrieu and Roberts 2009) with likelihoods estimated using sequential Monte Carlo (SMC) (Andrieu et al. 2010) to infer R_t trajectories. Specifically, we will use the particle marginal Metropolis–Hastings (PMMH) algorithm to propose parameters and latent prevalence trajectories.

There are a few methods using PMMH to combine prevalence data with (phylo)genetic data, most notably Rasmussen et al. 2011. The key difference with our method is it supposes that the prevalence and genomic data are related to each other, rather than independent of one another. We have also built in considerably more adaptation into our procedures to avoid computationally expensive hand-tuning of MCMC.

1.1 Phylogenetics

A phylogenetic tree or phylogeny is a diagram that represents evolutionary history. For an infectious disease, leaves denote sampled pathogens and internal nodes denote most recent common ancestors between those pathogens. A dated phylogeny uses a time scale rather than evolutionary scale. In a dated phylogeny, leaves are aligned with the known date of isolation of the genomes and nodes are aligned with the estimated dates of common ancestors. Many methods exist to reconstruct dated phylogenies from sampled sequence data, including BEAST (Suchard et al. 2018), BEAST2 (Bouckaert et al. 2019), LSD (To et al. 2016), BactDating (Didelot et al. 2018), treedater (Volz and Frost 2017) and TreeTime (Sagulenko et al. 2018).

A common analytical approach in the literature when using phylogenetic trees for inference is to first reconstruct a dated phylogenetic tree from sequencing data and to then draw some epidemiological interpretation from it (Didelot and Parkhill 2022). This is the approach that we take. Whilst this does not fully incorporate the uncertainty in the phylogenetic tree into the modelling, it does allow for considerable scalability, thus allowing us to take advantage of the abundance of genetic data.

We use coalescent theory to model the phylogeny (Kingman 1982) extended to allow for heterochronous sampling and a natural time scale (Drummond et al. 2002). The coalescent is robust to temporal bias in the genetic sampling as it models the ancestry given the sampling dates (Volz and Frost 2014). This is unlike methods modelling phylogenies as birth-death processes as these model both the branching and the sampling (Stadler 2009, Stadler 2010). Unlike the epidemiological data for which we have to assume the reporting probability is constant through time, there is no such assumption for the genetic data.

Several methods exist to estimate the effective population size over time given a dated tree (Ho and Shapiro 2011; Karcher et al. 2017; Volz and Didelot 2018; Didelot et al. 2023). However, this is not the same as estimating R_t . There is a complex relationship, not simply a proportional one, between the effective population size and the prevalence (Volz et al. 2009; Frost and Volz 2010; Volz 2012). We will discuss how to relate the effective population size to R_t in Section 2.3.

2 Bayesian modelling

2.1 Latent epidemic model

The epidemiological process considered is a non-homogeneous birth-death process (Kendall 1948). Modelling the epidemic in this way is akin to a susceptible-infectious-susceptible compartmental model with infinite population, so has been chosen for its simplicity and convenience.

The transition probabilities given by

$$\begin{aligned}
\mathbb{P}(X_{t+h} - X_t = 1 \mid X_t = i) &= \beta_t i h + o(h) \\
\mathbb{P}(X_{t+h} - X_t = -1 \mid X_t = i) &= \gamma_t i h + o(h) \\
\mathbb{P}(|X_{t+h} - X_t| > 1 \mid X_t = i) &= o(h) \\
\mathbb{P}(X_{t+h} - X_t = 0 \mid X_t = i) &= 1 - (\beta_t + \gamma_t) i h + o(h)
\end{aligned} \tag{1}$$

where $h \rightarrow 0$ is a small interval, β_t is the birth rate and γ_t is the death rate at time t .

We will suppose that the death rate $\gamma_t \equiv \gamma$ is constant and known. This model is shown in Figure 1.

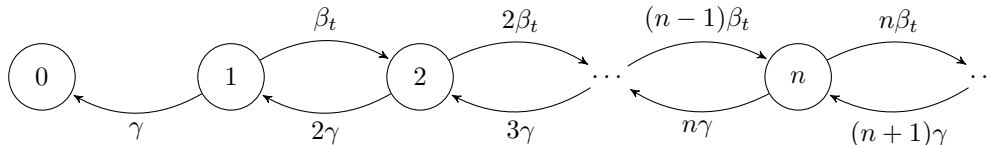


Figure 1: The number of infected in a population can be modelled as a time-inhomogeneous birth-death process with unknown birth rate β_t and known, constant death rate γ .

In a birth-death model of disease outbreak,

$$R_t = \frac{\beta_t}{\gamma_t} = \frac{\beta_t}{\gamma}. \tag{2}$$

Therefore, inferring β_t will allow us to infer R_t .

Whilst the underlying epidemic process is a continuous-time Markov process, we will only be observing it in discrete time, as we will have access to the prevalence for each unit of time. Note that these time units could be any arbitrary time step, but we will refer to one unit of time as a day throughout. In discrete time, for an epidemic that has been ongoing for N days, we are interested in modelling $p(X_{1:N} \mid X_0, \beta_{1:N}, \gamma) = \prod_{n=1}^N p(X_n \mid X_{n-1}, \beta_n, \gamma)$. Using rates given by setting $h = 1$ and ignoring the $o(h)$ terms in the transition probabilities in equation (1), we model birth events on day n as Poisson distributed with rate $\beta_n x_{n-1}$ and death events as Poisson distributed with rate γx_{n-1} when there are x_{n-1} infectious individuals on day $n - 1$. This is a natural and statistically convenient way to model the continuous-time birth-death process in discrete time. The difference between two (conditionally independent) Poisson distributions is given by the Skellam distribution (Skellam 1946), so we use this to calculate $p(X_{1:N} \mid X_0, \beta_{1:N}, \gamma)$.

Let B_n be the random variable representing the birth events on day n and let D_n be the random variable representing the death events on day n . Then $B_n \mid X_{n-1} = x_{n-1}, \beta_n \sim \text{Poisson}(\beta_n x_{n-1})$ and $D_n \mid X_n = x_n, \gamma \sim \text{Poisson}(\gamma x_{n-1})$, so $B_n - D_n \mid X_{n-1} = x_{n-1}, \beta_n, \gamma \sim \text{Skellam}(\beta_n x_{n-1}, \gamma x_{n-1})$. Note that B_n and D_n are conditionally independent given x_{n-1} . The likelihood for the latent epidemic is:

$$\begin{aligned}
p(X_{1:N} = x_{1:N} \mid X_0 = x_0, \beta_{1:N}, \gamma) &= \prod_{n=1}^N \mathbb{P}(X_n = x_n \mid X_{n-1} = x_{n-1}, \beta_n, \gamma) \\
&= \prod_{n=1}^N \mathbb{P}(B_n - D_n = x_n - x_{n-1} \mid X_{n-1} = x_{n-1}, \beta_n, \gamma) \\
&= \prod_{n=1}^N e^{-(\beta_n + \gamma)x_{n-1}} \left(\frac{\beta_n}{\gamma} \right)^{\frac{x_n - x_{n-1}}{2}} I_{|x_n - x_{n-1}|}(2x_{n-1} \sqrt{\beta_n \gamma})
\end{aligned} \tag{3}$$

where I is the modified Bessel function of the first kind.

This likelihood should ideally be conditioned to put probability 1 on the event that the epidemic does not die out, i.e. $B_n - D_n \mid X_{n-1} = x_{n-1}, \beta_n, \gamma \sim \text{Skellam}(\beta_n x_{n-1}, \gamma x_{n-1}) \mid B_n - D_n > -x_{n-1}$. However, this conditioning is computationally expensive and the probability of sampling below $-x_{n-1}$ is small, especially as the epidemic grows. As such, we ignore the condition in practice.

2.2 Epidemic observation model

We next consider how to model the observed epidemic given the latent epidemic and reporting probability, $p(Y_{1:N} \mid X_{1:N}, \rho) = \prod_{n=1}^N p(Y_n \mid X_n, \rho)$. There are many possible ways to model observed prevalence given latent prevalence depending on what you believe you are observing, for example, complete prevalence data with noise or partial cases. We will suppose that we are observing some proportion ρ of cases at random, i.e. $Y_n \mid X_n = x_n, \rho \sim \text{Binomial}(x_n, \rho) \forall n = 1, \dots, N$. X_n and ρ are conditionally independent given Y_n .

2.3 Phylogenetic model

Lastly, we consider how to model the dated phylogeny, inferred from sequencing data, given the birth rates and latent prevalence. The (exponential) rate at which coalescence events occur, denoted by λ_t , is given by (Koelle and Rasmussen 2012)

$$\lambda_t = \binom{A_t}{2} \frac{1}{N_e(t)} \quad (4)$$

where A_t denotes the number of lineages and $N_e(t)$ denotes the effective population size at time t . The effective population size reflects the number of individuals which contribute offspring to the descendent generation and is almost always smaller than the census population size (Ho and Shapiro 2011). Volz 2012 showed that for a phylogeny with A_t lineages, the coalescence rate can be written as a function of incidence f_t and population size X_t :

$$\lambda_t = f_t \frac{\binom{A_t}{2}}{\binom{X_t}{2}} \approx \binom{A_t}{2} \frac{2f_t}{X_t^2}. \quad (5)$$

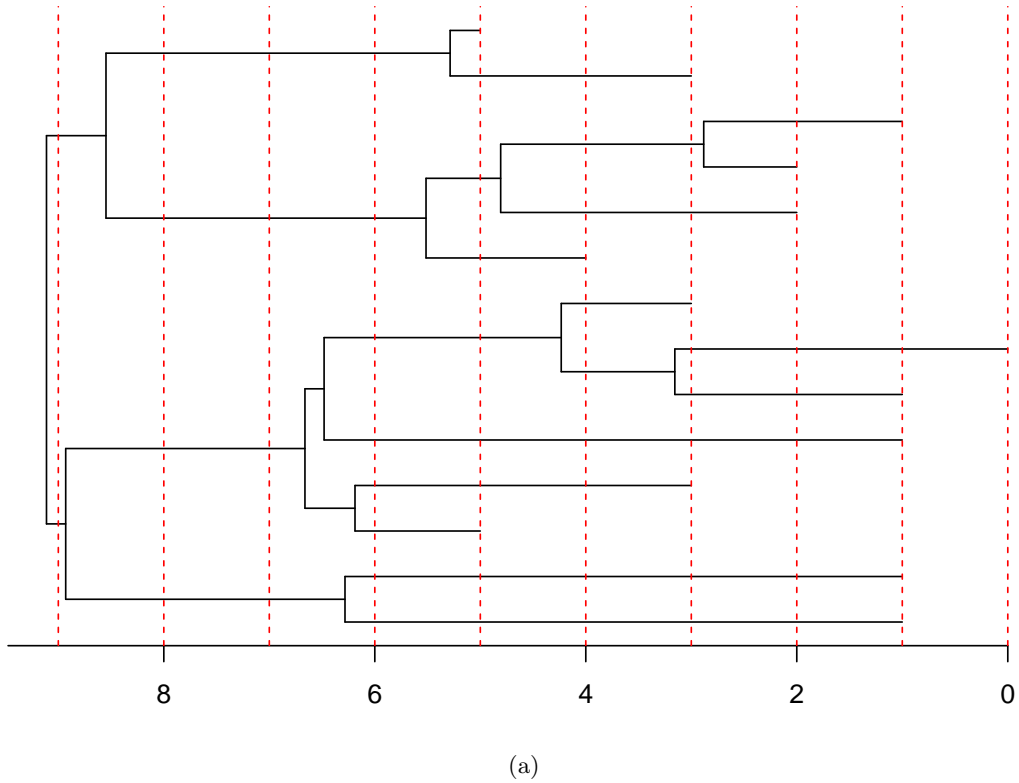
In a birth-death model of disease outbreak, the incidence $f_t = \beta_t X_t$, so

$$\lambda_t \approx \binom{A_t}{2} \frac{2\beta_t}{X_t}. \quad (6)$$

Since X_t is a process we infer in discrete time, it is therefore natural to also segment the dated phylogeny (see Figure 2). We do this by slicing the phylogeny into days, starting with the present day, and going backwards in time. On each day n , we have some number of lineages denoted A_n and some number of coalescence events C_n .

From (6) we know that coalescence events on day n occur at rate $\binom{A_n}{2} 2\beta_n / X_n$. This means each pair of lineages A_n coalesce at (exponential) rate $2\beta_n / X_n$. We model the number of coalescences as a binomial distribution with $\binom{A_n}{2}$ trials and success probability $1 - \exp(-2\beta_n / X_n)$. The likelihood for the dated phylogeny is therefore:

$$\begin{aligned} p(G_{1:N} \mid \beta_{1:N}, X_{1:N}) &= \prod_{n=1}^N p(G_n \mid \beta_n, X_n) \\ &= \prod_{n=1}^N p(C_n = c_n \mid A_n = a_n, \beta_n, X_n = x_n) \\ &= \prod_{n=1}^N \binom{\binom{a_n}{2}}{c_n} \left(1 - \exp\left(-\frac{2\beta_n}{X_n}\right)\right)^{c_n} \exp\left(-\frac{2\beta_n}{X_n}\right)^{\binom{a_n}{2} - c_n}. \end{aligned} \quad (7)$$



(a)

Days from the present	10	9	8	7	6	5	4	3	2	1	0
A_n	-	2	4	4	8	10	10	10	8	6	1
C_n	-	1	2	0	4	2	2	1	1	0	0

(b)

Figure 2: (a) A phylogenetic tree segmented by days from the present. (b) A table showing the corresponding values of A_n and C_n

2.4 State space model

Suppose the epidemic has been ongoing for N days. The aim is to infer the unknown birth rate trajectory $\beta_{1:N}$ given the segmented dated phylogeny $G_{1:N}$ and the partially observed epidemic $Y_{1:N}$. Since the epidemic has been observed discretely and we are discretising all other processes, we can present this in a state space model framework as seen in Figure 3.

Let β_n denote the birth rate on day n , G_n denote the slice of the phylogenetic tree from day $n - 1$ to n , X_n denote the latent prevalence on day n and Y_n denote the observed prevalence on day n . Let σ denote the amount that the birth rate trajectory is allowed to vary between days (details in Section 4.1) and let ρ denote the reporting probability, that is, the proportion of cases that have been observed.

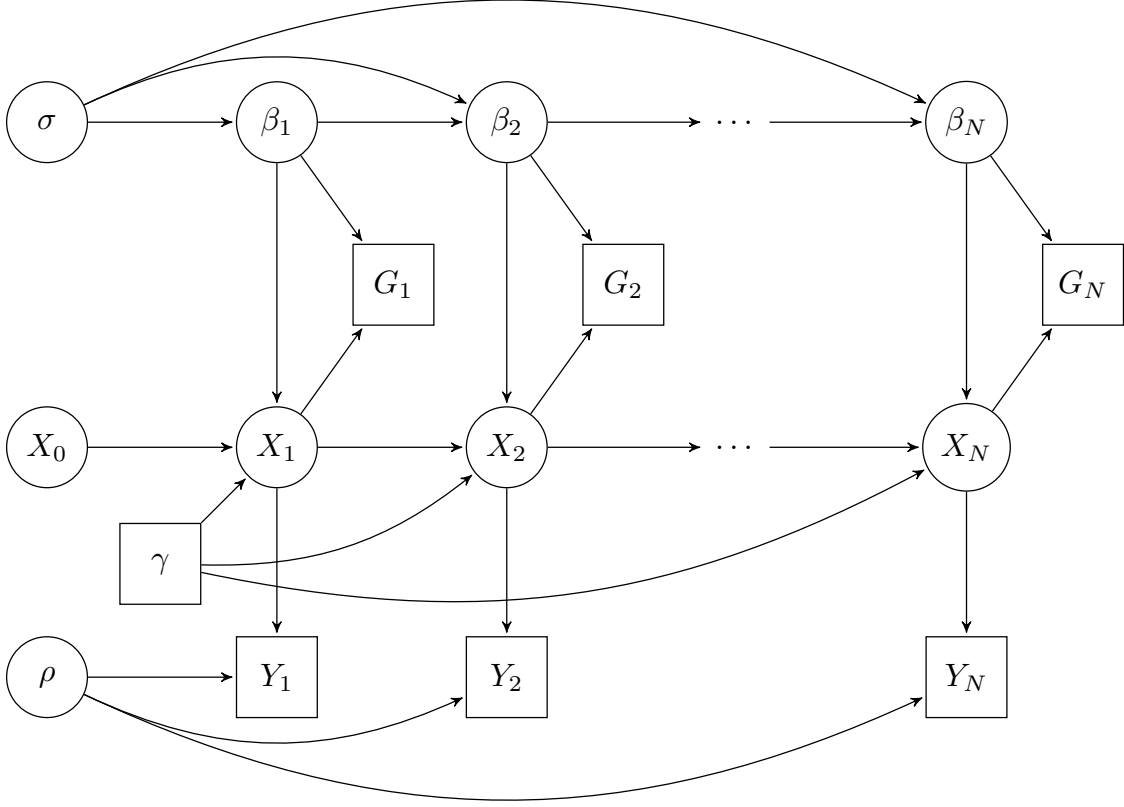


Figure 3: Bayesian network representing the conditional dependencies between the birth rates β_n , true prevalence X_n , genetic data G_n , observed prevalence Y_n on days $n = \{1, \dots, N\}$, the death rate γ and hyper-parameters σ and ρ . Square nodes denote observed variables and circular nodes denote unobserved variables.

We adopt a Bayesian approach to find $p(\beta_{1:N}, \sigma, \rho, X_0 \mid \gamma, G_{1:N}, Y_{1:N})$.

$$\begin{aligned}
& p(\beta_{1:N}, \sigma, \rho, X_0 \mid \gamma, G_{1:N}, Y_{1:N}) \\
& \propto p(\beta_{1:N}, \sigma, \rho, X_0, \gamma, G_{1:N}, Y_{1:N}) \\
& = \int p(\beta_{1:N}, \sigma, \rho, X_0, \gamma, G_{1:N}, Y_{1:N}, X_{1:N}) dX_{1:N} \\
& = \underbrace{p(\sigma)p(\rho)}_{\text{hyper-parameters}} \underbrace{p(X_0)}_{\text{birth rates}} \underbrace{p(\beta_{1:N} \mid \sigma)}_{\text{latent epidemic}} \int \underbrace{p(X_{1:N} \mid X_0, \beta_{1:N}, \gamma)}_{\text{phylogeny}} \underbrace{p(G_{1:N} \mid \beta_{1:N}, X_{1:N})}_{\text{observed epidemic}} \underbrace{p(Y_{1:N} \mid X_{1:N}, \rho)}_{\text{observed epidemic}} dX_{1:N}
\end{aligned} \tag{8}$$

The problem is that to evaluate this explicitly requires integrating over the space of all possible epidemics, which grows in the length of the time series. This is not analytically tractable. We will discuss methods to tackle this problem in Section 3. The rest of this section will present the models used to relate the data and the parameters.

3 Particle MCMC

3.1 Pseudo-marginal MCMC

As mentioned in the previous section, the distribution that we wish to target, $p(\beta_{1:N}, \sigma, \rho, X_0 \mid \gamma, G_{1:N}, Y_{1:N})$, is intractable. This prevents us from directly using standard likelihood-based infer-

ence tools, such as the Metropolis–Hastings algorithm (Hastings 1970), as we cannot evaluate the likelihood for each value of parameters σ , ρ and X_0 .

One approach to get around this could be data-augmented MCMC, where we augment the state space with the latent prevalence $X_{1:N}$ and the birth rate trajectory $\beta_{1:N}$ (Dyk and Meng 2001). However, since we are considering time series data, this method would vastly increase the number of variables over which to explore. Moreover, these variables would be highly correlated as future days in the time series depend upon previous ones. As such, these chains would be difficult to tune and mixing would likely be poor, and thus would need to be run for a very long time.

Instead we turn to a different class of MCMC methods called pseudo-marginal methods (Andrieu and Roberts 2009). In pseudo-marginal MCMC, we use an unbiased estimator of the analytically intractable likelihood, $\hat{p}(\beta_{1:N}, \sigma, \rho, X_0 \mid \gamma, G_{1:N}, Y_{1:N})$, in place of the true likelihood, $p(\beta_{1:N}, \sigma, \rho, X_0 \mid \gamma, G_{1:N}, Y_{1:N})$, in the Metropolis–Hastings algorithm. We do this by simulating several possible $X_{1:N}$ and $\beta_{1:N}$ for fixed hyper-parameters σ , ρ and X_0 , and then using these samples to estimate the likelihood of the data given these samples. We will derive this estimated likelihood using SMC, so specifically we will use the PMMH algorithm (Andrieu et al. 2010).

We target an acceptance rate of 10% using the adaptive scaling within adaptive Metropolis algorithm from Vihola 2011. This is close to optimal values demonstrated in Sherlock et al. 2015.

3.2 Sequential Monte Carlo

It is natural with time series data to want to sample sequentially in order to best exploit the structure of the data. For example, we know that the prevalence on day n depends on the prevalence on day $n - 1$, so we would like to sample the prevalence on day n given the prevalence on day $n - 1$. We can take advantage of this sequential sampling if on each day n we resample in order to keep the most likely proposals. This idea is the basis for SMC algorithms (Doucet and Johansen 2011).

Algorithm 1 SMC

Input: Values for hyper-parameters $\theta = (\sigma, \rho, X_0)$, number of particles K , death rate γ , observed prevalence data $Y_{1:N}$, discretised phylogenetic tree $G_{1:N}$

Output: L^K - an estimator for $\int p(\beta_{1:N}, X_{1:N}, G_{1:N}, Y_{1:N} \mid \theta, \gamma) dX_{1:N}$

for $n = 1, \dots, N$ **do**

Draw $(\beta_n^k, X_n^k) \sim q_\theta(\cdot \mid \beta_{1:n-1}^k, X_{1:n-1}^k)$ for $k = 1, \dots, K$

Weight the pairs (β_n^k, X_n^k) as

$$w_n^k = \frac{p_\theta(\beta_{1:n}^k, X_{1:n}^k, G_{1:n}, Y_{1:n})}{p_\theta(\beta_{1:n-1}^k, X_{1:n-1}^k, G_{1:n-1}, Y_{1:n-1})q_\theta(\beta_n^k, X_n^k \mid \beta_{1:n-1}^k, X_{1:n-1}^k)}$$

Normalise $W_n^k = w_n^k / \sum_{j=1}^K w_n^j$

Resample ancestors $A_n^{1:K}$ according to the normalised weights and keep pairs $(\beta_n^{A_n^{1:K}}, X_n^{A_n^{1:K}})$

Set $l_n^K = \frac{1}{K} \sum_{k=1}^K w_n^k$

Set $w_n^k = 1$

end for

Set $L_n^K = \prod_{t=1}^n l_t^K$ **return** L_N^K

The resampling step will be discussed in more detail in Section 3.4.1. If desired, we can also output samples of trajectories $\beta_{1:N}$ and/or $X_{1:N}$ by choosing a trajectory according to its weight at step N and outputting that.

3.3 Particle marginal Metropolis–Hastings

Let us denote by \hat{p}_{SMC} the estimator for the likelihood from using the SMC algorithm. The PMMH algorithm is a specific kind of pseudo-marginal sampler where the unbiased estimator used is \hat{p}_{SMC} .

Algorithm 2 PMMH

Input: Initial values $\theta^{(0)}$ for unknown hyper-parameters $(\sigma^{(0)}, \rho^{(0)}, X_0^{(0)})$, number of iterations I , number of particles K , death rate γ , observed prevalence data $Y_{1:N}$, phylogenetic tree G

Output: σ - a vector of length I , ρ - a vector of length I , \mathbf{X}_0 - a vector of length I , β - a matrix with dimension $I \times N$

Run the SMC algorithm targeting $f(\beta_{1:N}^{(0)}, X_{1:N}^{(0)} \mid \theta^{(0)}, \gamma, Y_{1:N}, G)$, simulate K pairs of trajectories $(\beta_{1:N}^{(0)}, X_{1:N}^{(0)})$ and compute $\hat{p}_{\text{SMC}}(\beta_{1:N}^{(0)}, X_{1:N}^{(0)} \mid \theta^{(0)}, \gamma, Y_{1:N}, G)$

for $i = 1, \dots, I$ **do**

Draw $\theta^* \sim q(\cdot \mid \theta^{(i-1)})$

Run the SMC algorithm targeting $f(\beta_{1:N}^*, X_{1:N}^* \mid \theta^*, \gamma, Y_{1:N}, G)$, simulate K pairs of trajectories $(\beta_{1:N}^*, X_{1:N}^*)$ and compute $\hat{p}_{\text{SMC}}(\beta_{1:N}^*, X_{1:N}^* \mid \theta^*, \gamma, Y_{1:N}, G)$

Compute the ratio $r = \frac{p(\theta^*)\hat{p}_{\text{SMC}}(\beta_{1:N}^*, X_{1:N}^* \mid \theta^*, \gamma, Y_{1:N}, G)q(\theta^{(i-1)} \mid \theta^*)}{p(\theta^{(i-1)})\hat{p}_{\text{SMC}}(\beta_{1:N}^{(i-1)}, X_{1:N}^{(i-1)} \mid \theta^{(i-1)}, \gamma, Y_{1:N}, G)q(\theta^* \mid \theta^{(i-1)})}$

Draw $u \sim \text{Uniform}(0, 1)$

if $u \leq \min\{1, r\}$ **then**

$\theta^{(i)} = \theta^*$

$(\beta_{1:N}^{(i)}, X_{1:N}^{(i)}) = (\beta_{1:N}^*, X_{1:N}^*)$

$\hat{p}_{\text{SMC}}(\beta_{1:N}^{(i)}, X_{1:N}^{(i)} \mid \theta^{(i)}, \gamma, Y_{1:N}, G) = \hat{p}_{\text{SMC}}(\beta_{1:N}^*, X_{1:N}^* \mid \theta^*, \gamma, Y_{1:N}, G)$

else

$\theta^{(i)} = \theta^{(i-1)}$

$(\beta_{1:N}^{(i)}, X_{1:N}^{(i)}) = (\beta_{1:N}^{(i-1)}, X_{1:N}^{(i-1)})$

$\hat{p}_{\text{SMC}}(\beta_{1:N}^{(i)}, X_{1:N}^{(i)} \mid \theta^{(i)}, \gamma, Y_{1:N}, G) = \hat{p}_{\text{SMC}}(\beta_{1:N}^{(i-1)}, X_{1:N}^{(i-1)} \mid \theta^{(i-1)}, \gamma, Y_{1:N}, G)$

end if

$\sigma[i,] = \sigma^{(i)}$

$\rho[i,] = \rho^{(i)}$

$\mathbf{X}_0[i,] = X_0^{(i)}$

Sample one trajectory $\beta_{1:N}^k$ from $\beta_{1:N}^{(i)}$

$\beta[i,] = \beta_{1:N}^k$

end for

return $\sigma, \rho, \mathbf{X}_0, \beta$

3.3.1 Proposal mechanisms

The birth rates are sampled according to their prior. That is, the birth rate on the first day is supposed to be exponential with rate $(2\gamma)^{-1}$ and on subsequent days are normal centred on the previous birth rate with variance σ^2 .

Values for the latent prevalence are sampled from a mixture distribution of the Skellam prior and a proposal distribution informed by the data. The balance of the mixture is chosen depending on the reporting probability ρ . Given ρ , we propose $x_n \sim p \cdot \text{NegBin}(y_n, \rho) + (1 - p) \cdot \text{Skellam}(\beta_n x_{n-1}, \gamma x_{n-1})$. In practice, we say $p = \min\{\rho/0.1, 0.95\}$, which gives a mixture proposal that is very data-driven, but also allows for the samples to take reasonable values when in the tails of the reporting probability space (i.e. when the data-driven proposals would be misleading).

3.4 Path degeneracy

As the length of the epidemic increases (i.e. as N increases), the resampling step in the SMC algorithm necessarily results in a phenomenon called path degeneracy, where all trajectories with

high weights on day N start from one sample on days $1, \dots, t$ for some $t < N$ (Doucet and Johansen 2011). This path degeneracy can lead to poor inference of the birth rate for earlier days of the epidemic. There are a few techniques to combat this path degeneracy which we will discuss in the rest of this section.

3.4.1 Resampling schemes

There are several options for the resampling step in the SMC algorithm, as the only constraint is that the resampling mechanism gives rise to an unbiased estimator of the likelihood. We use systematic resampling. In this resampling scheme, we sample an initial $U_1 \sim \text{Uniform}(0, 1/K)$ and set $U_i = U_1 + (i - 1)/K$. We then sample the particles for which the cumulative weights are between U_{i-1} and U_i . Systematic resampling empirically yields lower-variance estimates of the log-likelihood, slowing path degeneracy (Chopin and Papaspiliopoulos 2020).

3.4.2 Adaptive resampling

In Algorithm 1 resampling is performed in every step. However, we know that this resampling step introduces noise and reduces our number of useful particles. One such way to reduce this noise is to not resample in every step. Instead, we only resample if the number of useful particles, denoted by the effective sample size (ESS), falls below a threshold, conventionally set at $K/2$. ESS of normalised weights $W^{1:K}$ is given by:

$$\text{ESS}(W^{1:K}) = \frac{1}{\sum_{k=1}^K (W^k)^2} \quad (9)$$

Its interpretation as the number of useful particles is because if one particle has all the weight, then $\text{ESS} = 1$, and if all particles have equal weight, then $\text{ESS} = K$.

3.4.3 Backward simulation

Running the PMMH algorithm only requires unbiased likelihood estimators, but we are also interested in the realisations of the birth rate trajectories. These can be extracted from the SMC algorithm naively by tracking the history of one particle according to its weight on the last day. However, this is vulnerable to path degeneracy, as particles with high weight on the last day are often descendants of the same particles on early days. Therefore, the last strategy we employ to reduce the variance introduced by resampling is a method called backward simulation (Godhill et al. 2004).

Backward simulation is run backwards in time after the SMC algorithm. It re-weights samples to smooth out trajectories such that the samples of the birth rate and prevalence on each day $n \leq N$ are conditional on observations from all days $1, \dots, N$ rather than only historical days $1, \dots, n$. That is, rather than choosing a sample trajectory $\beta_{1:N}^k$ according to the weights on day N , we use backward simulation to sample a trajectory. We get this trajectory using the following steps:

1. Run the SMC algorithm forward-in-time, storing all particles and weights in each generation, even those culled by resampling.
2. Set $j_N = k$ with probability $w_N^k / \sum_l w_N^l$.
3. For $n = N - 1, \dots, 1$, compute the smoothing weights

$$w_{n|N}^k = \frac{w_n^k p(\beta_{n+1}^{j_{n+1}}, x_{n+1}^{j_{n+1}} | \beta_n^k, x_n^k)}{\sum_l w_n^l p(\beta_{n+1}^{j_{n+1}}, x_{n+1}^{j_{n+1}} | \beta_n^l, x_n^l)}.$$

4. Set $j_n = k$ with probability $w_{n|N}^k$.

Then our sample trajectory is $\{\beta_n^{j_n}\}$ for all $n = 1, \dots, N$. This path should be representative across the whole time series, rather than only a good fit at the end.

Empirical results showing the improvements from implementing systematic resampling, adaptive resampling and backward simulation can be seen in Appendix A.

3.5 Choosing the number of particles

We use the suggested guidance from Pitt et al. 2012 which proposes the following steps:

1. Run a short MCMC scheme with a large number of particles K to determine an approximate value for the posterior mean of θ , denoted $\bar{\theta}$.
2. Run the SMC algorithm for several (say $R = 100$) independent runs for a fixed starting value of particles K_s and obtain an estimator of the likelihood $\hat{p}_{K_s}^i(y | \bar{\theta})$, $i = 1, \dots, R$ for each.
3. Record the variance of the log of the likelihood estimator as

$$\hat{\sigma}^2(\bar{\theta}, K_s) = \frac{1}{R} \sum_{i=1}^R (\log \hat{p}_{K_s}^i(y | \bar{\theta}))^2 - \left(\frac{1}{R} \sum_{i=1}^R \log \hat{p}_{K_s}^i(y | \bar{\theta}) \right)^2.$$

4. Choose the optimal number of particles K_{opt} as

$$M_{opt} = K_s \times \frac{\hat{\sigma}^2(\bar{\theta}, K_s)}{0.92^2}.$$

0.92 is the number calculated in Pitt et al. 2012 which minimises the computing time of the pseudo-marginal MCMC algorithm. In practice we found that this method can be volatile, because step 1 does not always manage to find a good value for θ . We instead run this scheme three times and choose the maximum number of particles.

4 Simulation study

All trace plots and posterior density plots for hyper-parameters σ and X_0 for this section and the next section can be found in Appendix B. We used the scheme described in Section 3.5 to choose the number of particles. However, we imposed a cap of 5,000 particles. This cap on the number of particles is effectively a cap on computational cost, so this limits run time to around 1 day on a standard laptop.

4.1 Priors

The prior used for β_1 , the birth rate on the first day of the epidemic, is exponential with rate $(2\gamma)^{-1}$. This has mean 2γ to reflect a belief that the epidemic will be growing initially. The prior for $\beta_n | \beta_{n-1}, \sigma$ is a Folded-Normal(β_{n-1}, σ^2) for $n = 2, \dots, N$. The folded normal distribution is the distribution of the absolute value of a random variable with a normal distribution (Leone et al. 1961).

The prior used for σ is exponential with rate 10. This has a mean of 0.1 as we expect small changes in the birth rate between days.

The prior used for the reporting probability ρ is Uniform(0,1). This allows us to suppose that we have no notion of how much of the epidemic that we are observing.

The prior used for X_0 , the number of cases on day 0, is an improper Uniform(1,∞) prior.

4.2 Constant reproduction number

We first demonstrate simulation results in a simple scenario - a constant reproduction number. We have simulated an epidemic with a constant birth rate of $\beta_t = 0.3$ and a death rate of $\gamma = 0.1$ for 40 days. For many infectious diseases, the reporting probability is low. To mimic the case data we would have access to in practice, we take noisy observations from the true prevalence ranging from 1-5%. To mimic the phylogenetic data we would have access to, we put every case into a phylogenetic tree, and then take a sample of the historical leaves ranging from 1-5%. The observed prevalences and sampled phylogenies are shown in Figure 4.

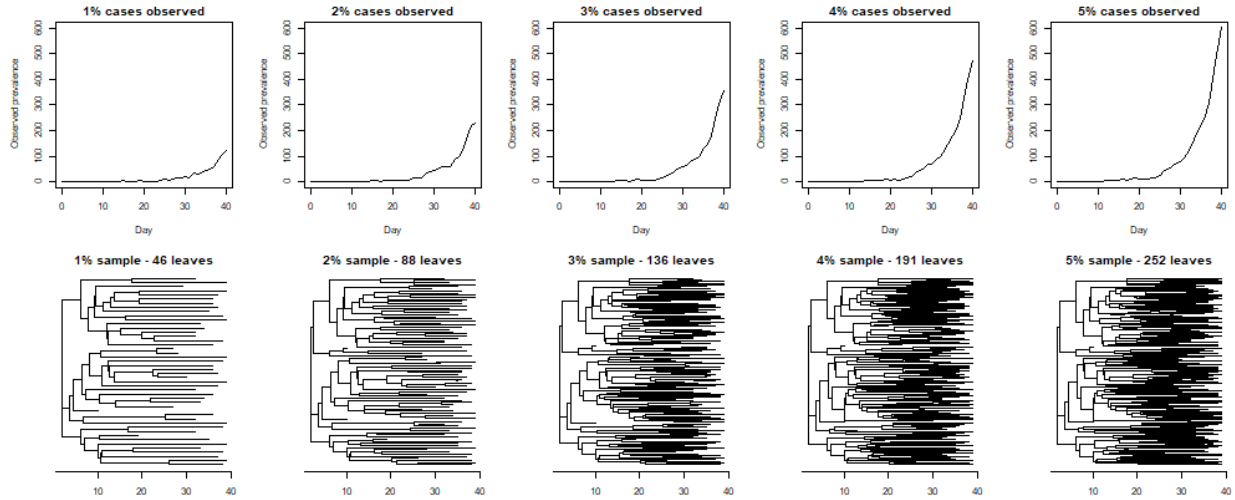


Figure 4: Observed prevalences and sampled phylogenies of a simulated epidemic with a constant birth rate.

For each sampling proportion from 0% to 5%, we have run the PMMH algorithm. All chains have been run for 100,000 iterations with initial values of $\sigma_0 = 0.1$, $\rho_0 = 0.5$ and $X_0 = 1$. Posterior density plots for ρ are shown in Figure 5. Note that the densities of ρ are omitted in the case of 0% epidemiological data, because we know $\rho = 0$ when there is no prevalence data. Inference plots for β_t are shown in Figure 6.

It is clear from the posterior density plots of ρ in Figure 5 that the inclusion of genetic data significantly improves the inference of the reporting probability compared to epidemiological data alone. For all scenarios, the posterior mean for ρ is closer to the true value than its prior mean of 0.5, and the shape of the distribution is clearly non-uniform, so all posteriors show learning from the data.

Figure 6 shows that in all cases, the combination of epidemic and genetic data seems to improve inference of the birth rate compared with only considering epidemiological data or genetic data alone. Epidemiological data alone has particularly wide credible intervals at the beginning of the epidemic as that is when there is least prevalence data. Genetic data alone has widest credible intervals at the end of the epidemic, because the salient information in the phylogeny are the coalescent events, and these don't occur until further back in the tree. Therefore, the combination of the sources of data allows for less uncertainty throughout the trajectory. It can also be seen that more genetic data (across) or more epidemiological data (down) generally reduces the uncertainty of the inference. There is variation however. For example, when there is 1% genetic data, the case of 1% of prevalence observed has narrower credible intervals than 2-4%.

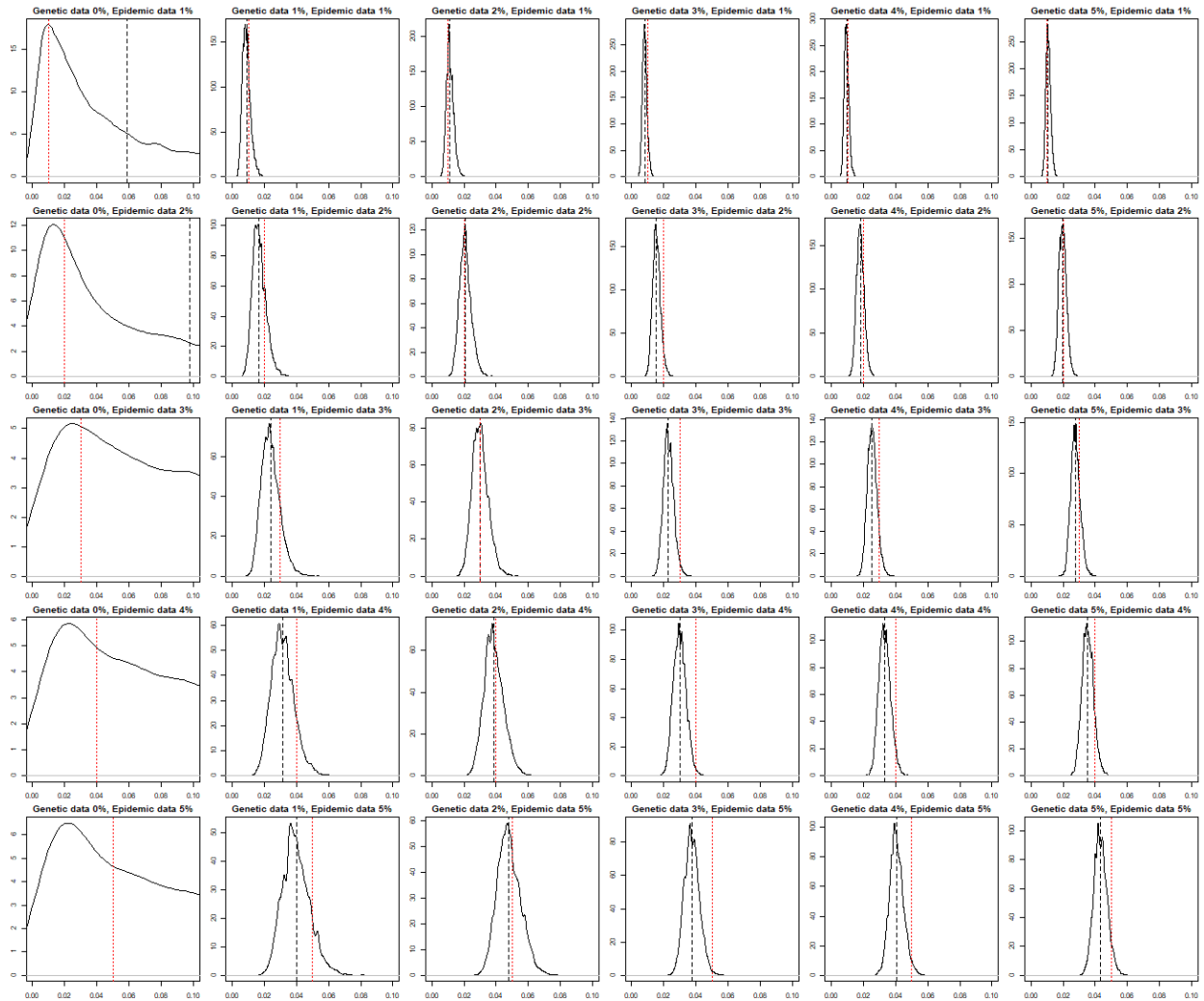


Figure 5: Posterior density of the reporting probability for a simulated epidemic with a constant birth rate. The dashed black line represents the posterior mean. The red dashed represents the true reporting probability.

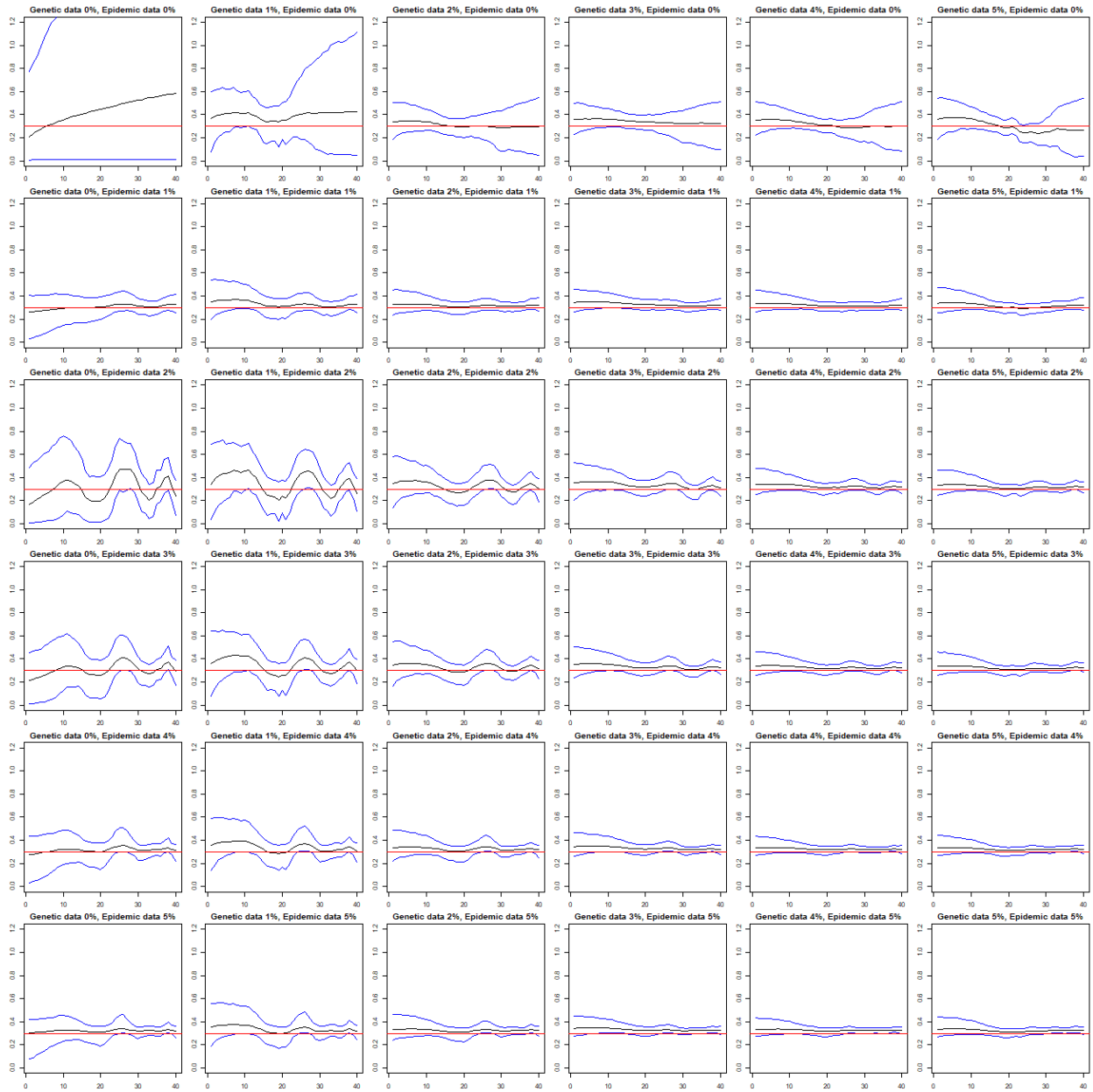


Figure 6: Inferred birth rates for a simulated epidemic with constant birth rate. The posterior mean is shown in black, the posterior 95% credible interval is shown in blue and the true trajectory is shown in red.

4.3 Peaked reproduction number

For our next scenario, we consider the most realistic possibility. That is, a reproduction number that is increasing and then decreasing. We have simulated an epidemic with a birth rate increasing linearly from 0.1 to 0.5 until midway through the epidemic and then decreasing linearly from 0.5 to 0.1, and a death rate of $\gamma = 0.1$ for 40 days. The observed prevalences and sampled phylogenies are shown in Figure 7.

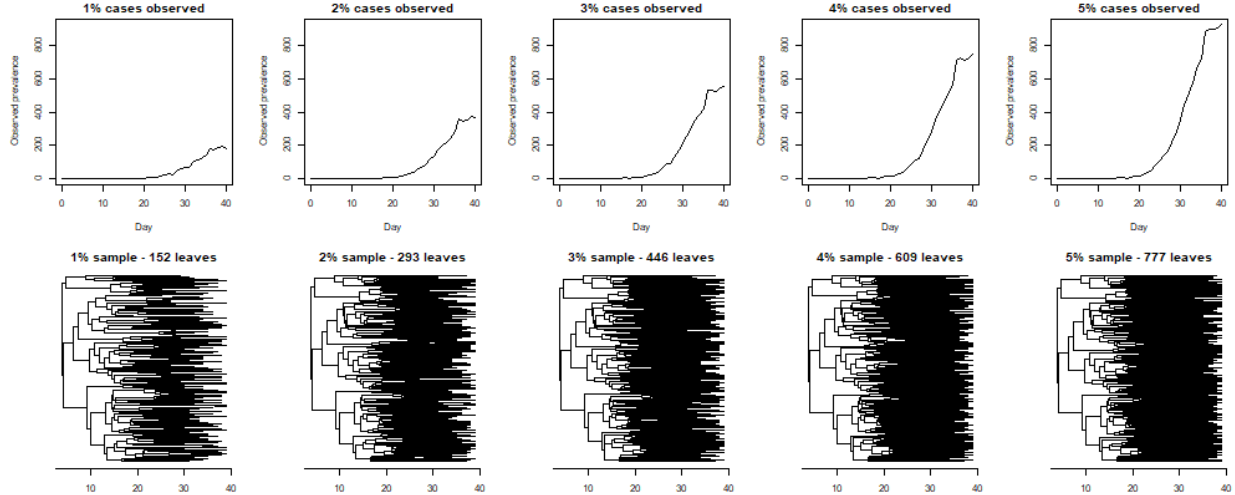


Figure 7: Observed prevalences and sampled phylogenies of a simulated epidemic with a peaked birth rate.

For each sampling proportion from 0% to 5%, we have run the PMMH algorithm. All chains have been run for 100,000 iterations with initial values of $\sigma_0 = 0.1$, $\rho_0 = 0.5$ and $X_0 = 1$. Posterior density plots for ρ are shown in Figure 8. Inference plots for β_t are shown in Figure 9.

As in the constant R_t simulation, it is clear from the posterior density plots of ρ in Figure 8 that the inclusion of genetic data improves the inference of the reporting probability compared to epidemiological data alone. In fact, more genetic data seems to improve inference of the reporting probability. For all scenarios, the posterior mean for ρ is closer to the true value than its prior mean of 0.5, and the shape of the distribution is clearly non-uniform, so all posteriors show learning from the data.

Figure 9 shows inference is poor across the board in the first half of the epidemic. In a peaked scenario, most genetic data is concentrated in the middle of the epidemic and most prevalence data is at the end of the epidemic, so it can be difficult to infer further back in time than midway. This concentration of genetic data in the middle of the epidemic can be seen in the first row of plots, where genetic data alone infers a fairly flat β_t around 0.5, the true value on day 20 of 40. Whilst the credible intervals for the combined data are smaller than single sources, they sometimes exclude the truth. The poor inference here seems to be driven by the fact that the genetic data on its own struggles to pick up a pattern in the reproduction number. However, the inference for days 20-40 of the epidemic is generally good, and improves with more data. Considering the complexity of the scenario, the inference is reasonable.

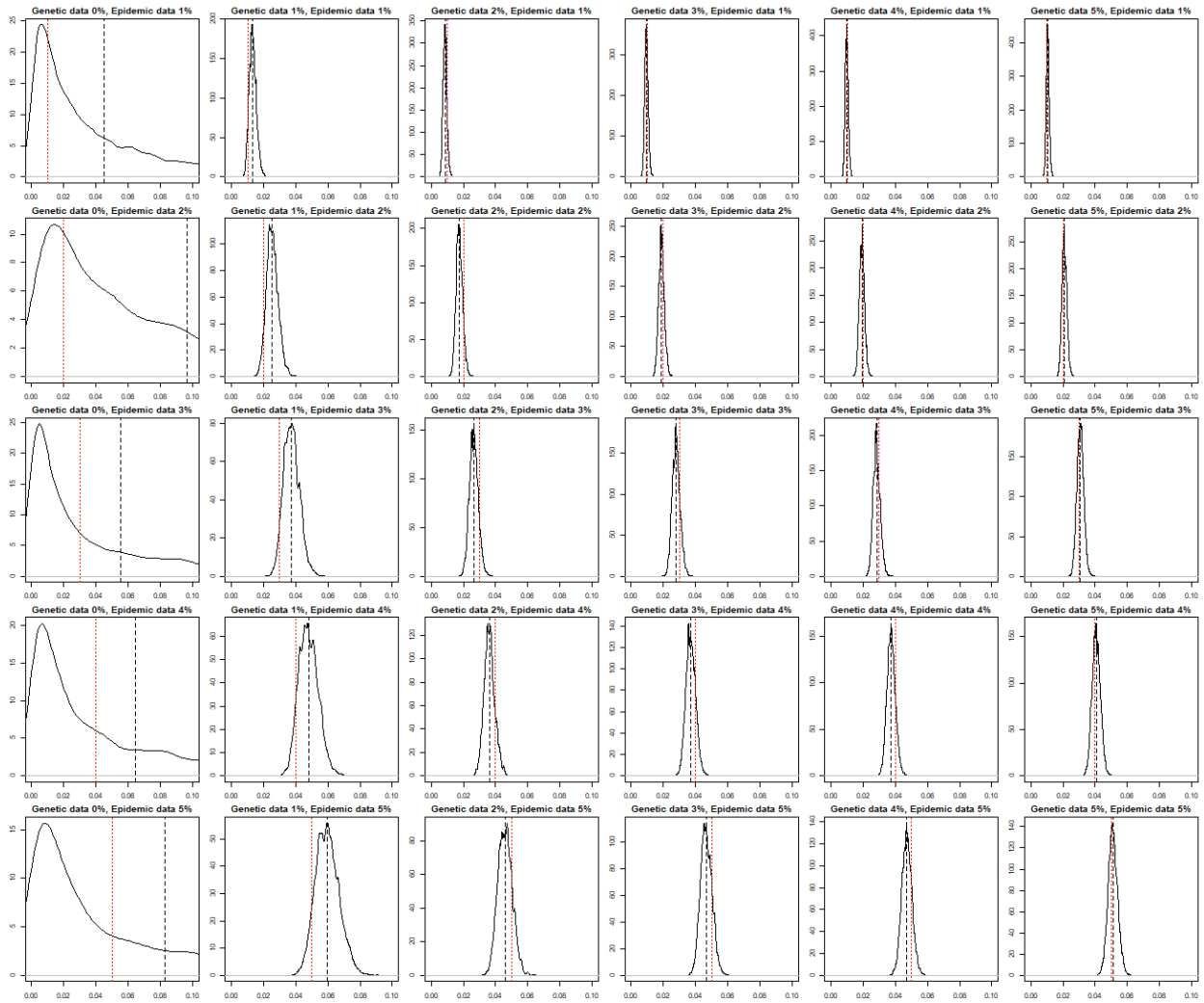


Figure 8: Posterior density of the reporting probability for a simulated epidemic with a peaked birth rate. The dashed black line represents the posterior mean. The red dashed represents the true reporting probability.

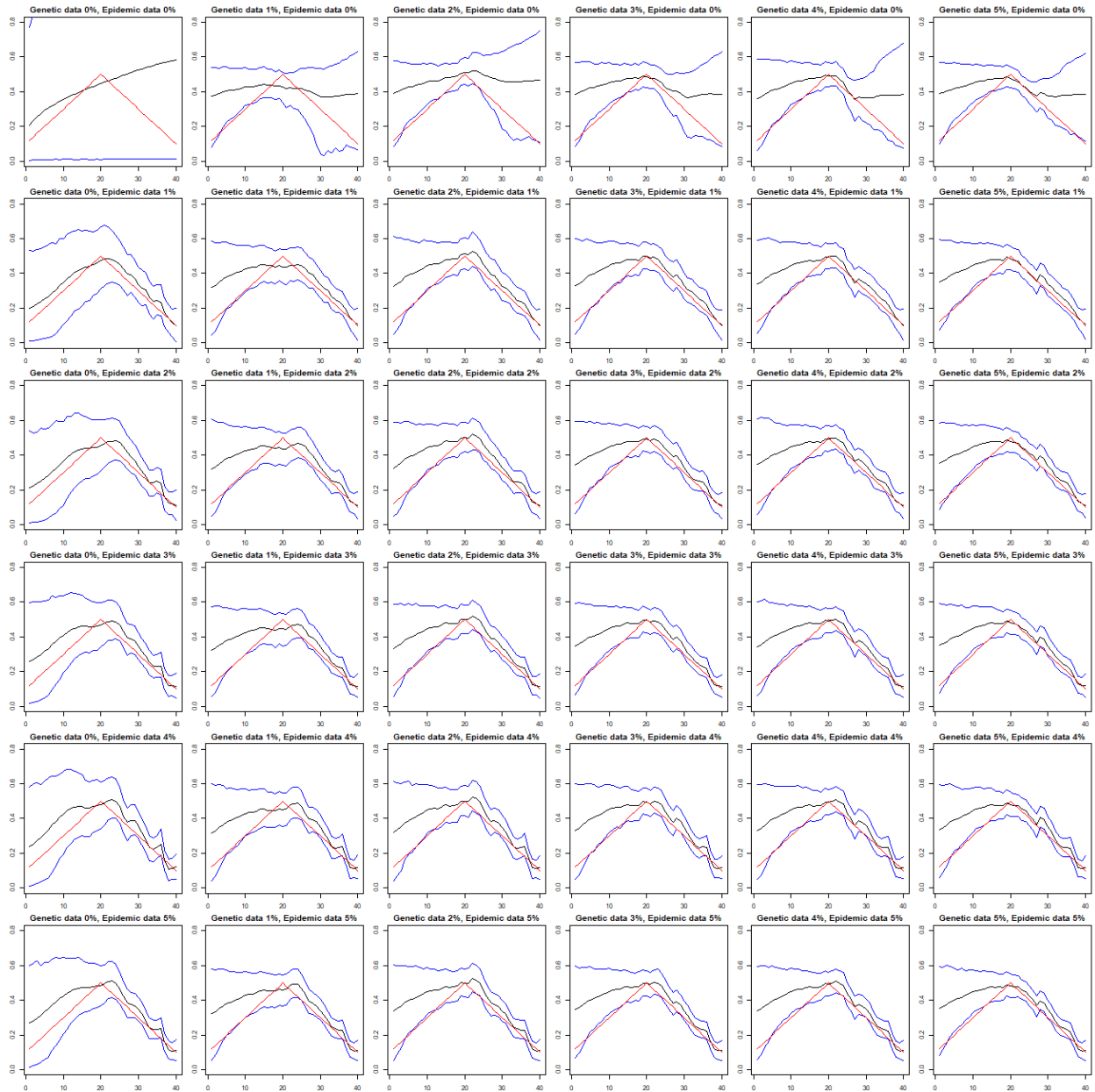


Figure 9: Inferred birth rates for a simulated epidemic with peaked birth rate. The posterior mean is shown in black, the posterior 95% credible interval is shown in blue and the true trajectory is shown in red.

4.4 Change point in reproduction number

For our final scenario, we deliberately consider a case which will be difficult for our method to resolve - a change point. The change point scenario is difficult for the model as we are supposing, via the hyper-parameter σ , that R_t varies smoothly through time. We have simulated an epidemic with a birth rate constant at 0.5 until midway through the epidemic and then constant at 0.1, and a death rate of $\gamma = 0.1$ for 40 days. The observed prevalences and sampled phylogenies are shown in Figure 10.

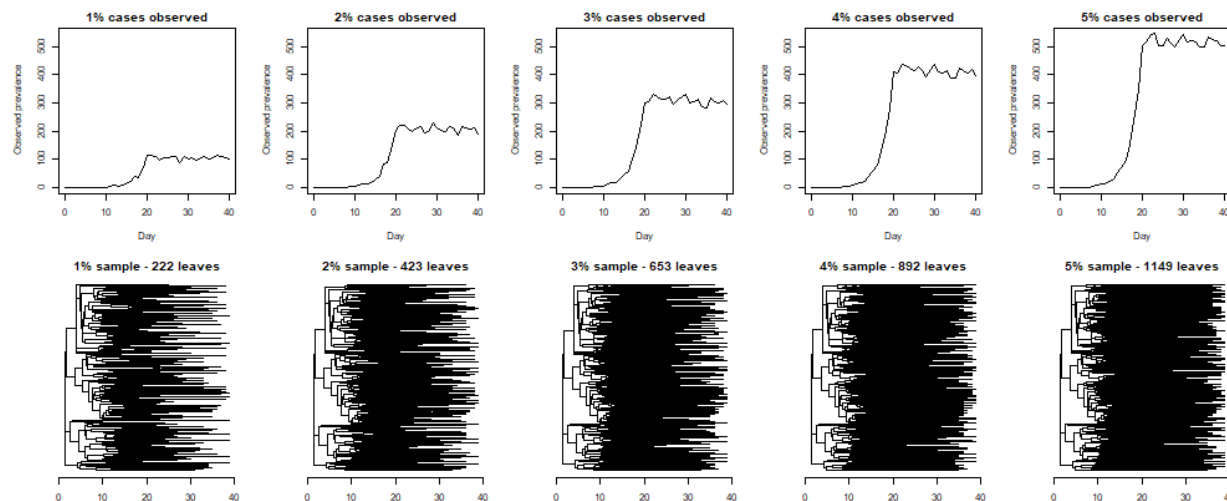


Figure 10: Observed prevalences and sampled phylogenies of a simulated epidemic with a change point in the birth rate.

For each sampling proportion from 0% to 5%, we have run the PMMH algorithm. All chains have been run for 100,000 iterations with initial values of $\sigma_0 = 0.1$, $\rho_0 = 0.5$ and $X_0 = 1$. Posterior density plots for ρ are shown in Figure 11. Inference plots for β_t are shown in Figure 12.

It is clear from the posterior density plots of ρ in Figure 11 that the inclusion of genetic data improves the inference of the reporting probability compared to epidemiological data alone. For all scenarios, the posterior mean for ρ is closer to the true value than its prior mean of 0.5, and the shape of the distribution is clearly non-uniform, so all posteriors show learning from the data.

Figure 12 shows inference is reasonable considering the complexity of the scenario, but similarly to the peaked R_t case, it struggles in the first half of the epidemic. This is unsurprising as early on in the epidemic has the least data. Unlike in the peaked reproduction number simulation, the genetic data on its own can generally detect the change point, so the combination of data allows for less uncertainty in the inference.

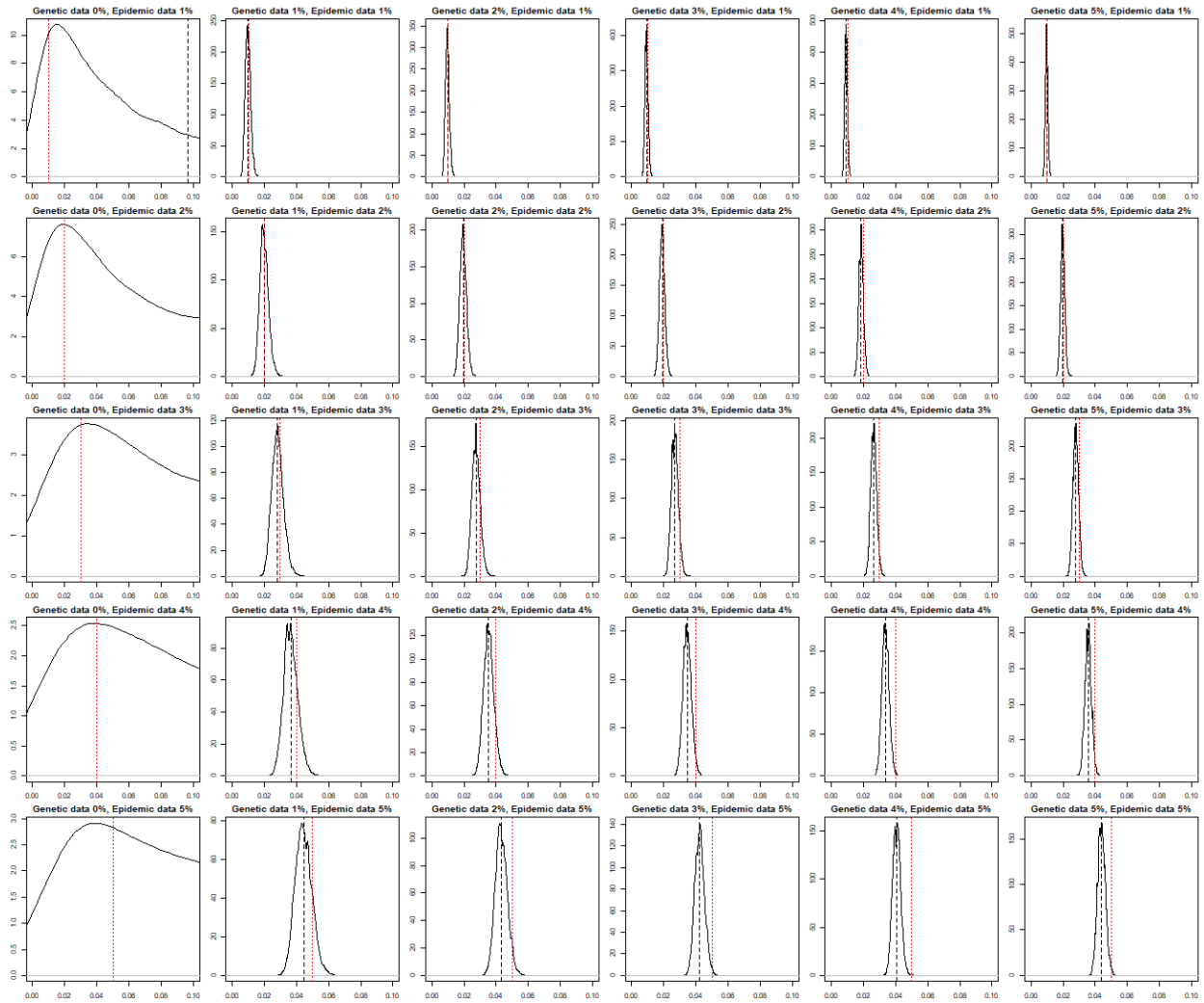


Figure 11: Posterior density of the reporting probability for a simulated epidemic with a change point in birth rate. The dashed black line represents the posterior mean. The red dashed represents the true reporting probability.

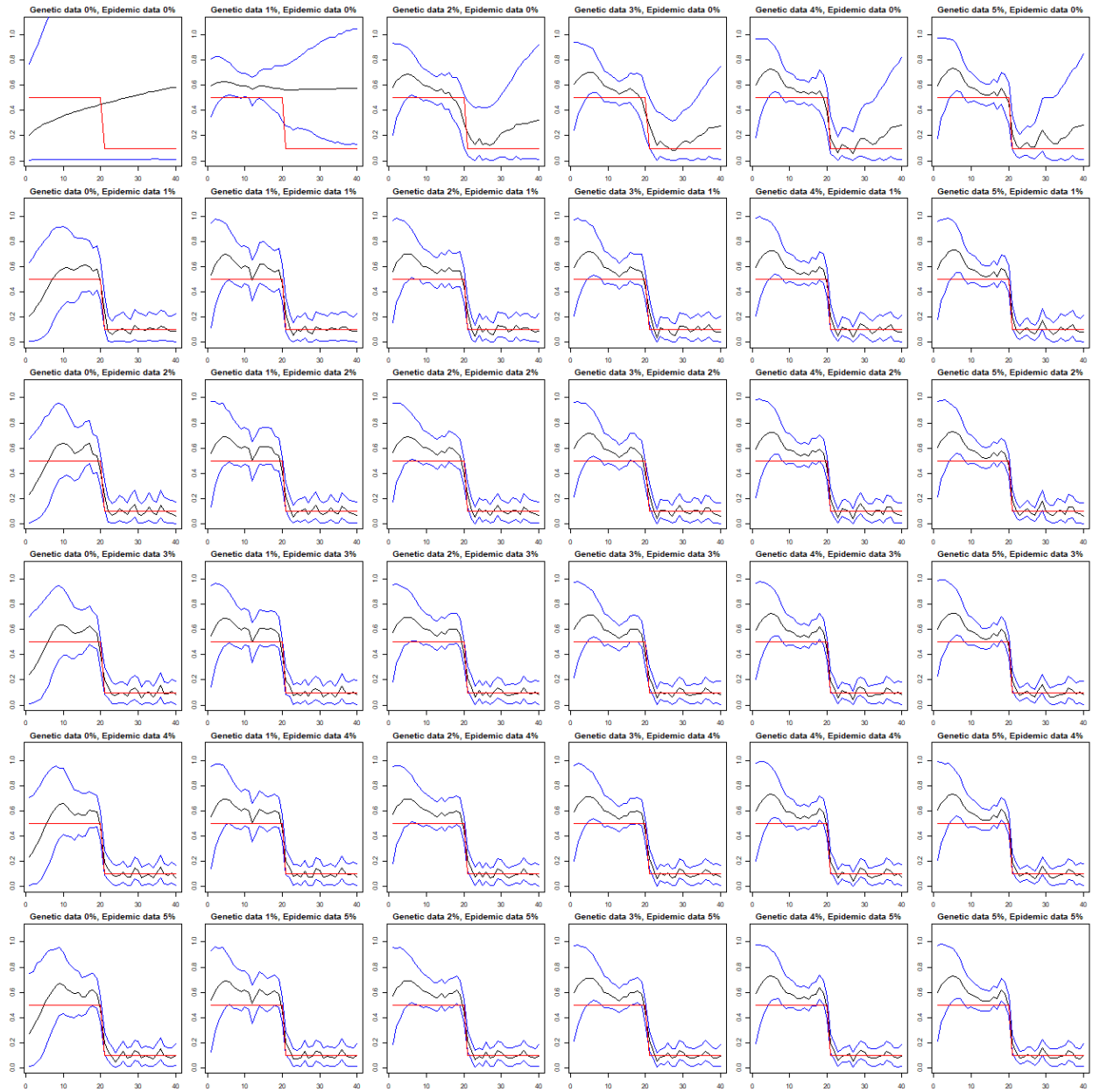


Figure 12: Inferred birth rates for a simulated epidemic with a change point in the birth rate. The posterior mean is shown in black, the posterior 95% credible interval is shown in blue and the true trajectory is shown in red.

5 Case study: HIV-1 in North Carolina, USA

Having verified the method in Section 4, we now consider a real data set. This data is of HIV-1 in North Carolina, USA. Sequences were sampled from 1997 to 2019 and the US Centers for Disease Control had estimates of the prevalence of HIV in North Carolina from 2010 to 2019. This data is from Didelot et al. 2023 and more details can be found there. The prevalence is shown in Figure 13 and the phylogenetic tree is shown in Figure 14.

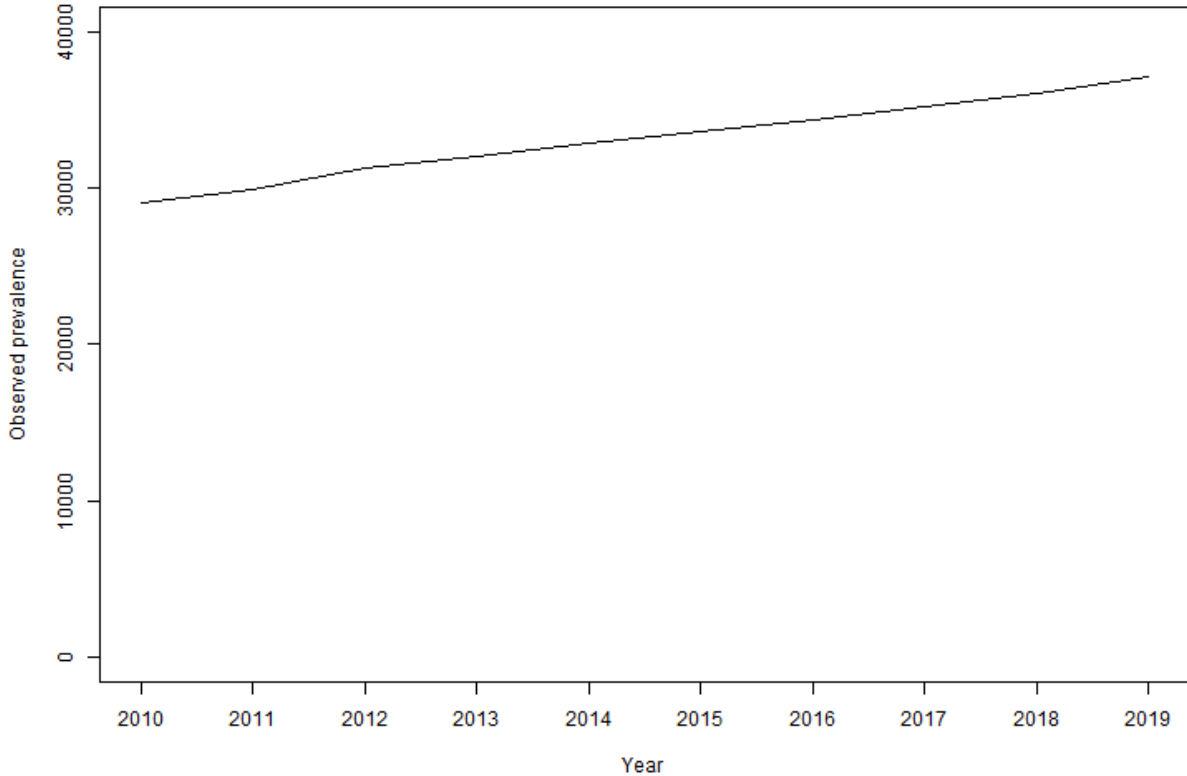


Figure 13: Prevalence of HIV-1 in North Carolina by year.

This phylogeny has 1850 leaves, which is very informative. Instead of using the full tree, we took a sub-sample of the tree, by sampling 5% of the leaves at random. The resulting phylogeny has 100 leaves. This sampled phylogenetic tree is shown in Figure 15.

The PMMH algorithm was run for 100,000 iterations. As in the simulations, we imposed a cap on the number of particles in order to cap the run time. Due to the possible complexity of a real data scenario and the increased length of the time-series compared to simulations, we have capped the number of particles at 10,000. Initial values used were $\rho_0 = 0.9$, $\sigma_0 = 0.1$ and $X_0 = 1$. $\rho_0 = 0.9$ is because we expect the reporting probability of HIV-1 from 2010 to 2019 to be high as it is a high profile disease that is regularly tested for. $\sigma_0 = 0.1$ was chosen as the prior mean to reflect no particular expectation. $X_0 = 1$ is because the length of the inference spans the length of the phylogeny and we expect that there were very few cases of HIV-1 when the phylogeny reaches a most recent common ancestor in 1957. The death rate used was $\gamma = 0.1$ to reflect a removal time of 10 years. The optimum number of particles chosen was 10,000 and the chain took 13 hours and 40 minutes to run. The target acceptance rate was 10% and the actual acceptance rate was 10%. The results of this inference can be seen in Figures 16 and 18.

The posterior densities of the hyper-parameters ρ , σ and X_0 all look considerably different to the priors, indicating that we have learned from the data. The reporting probability ρ and the day 0 prevalence X_0 look especially different from their uniform priors. The posterior mean of the

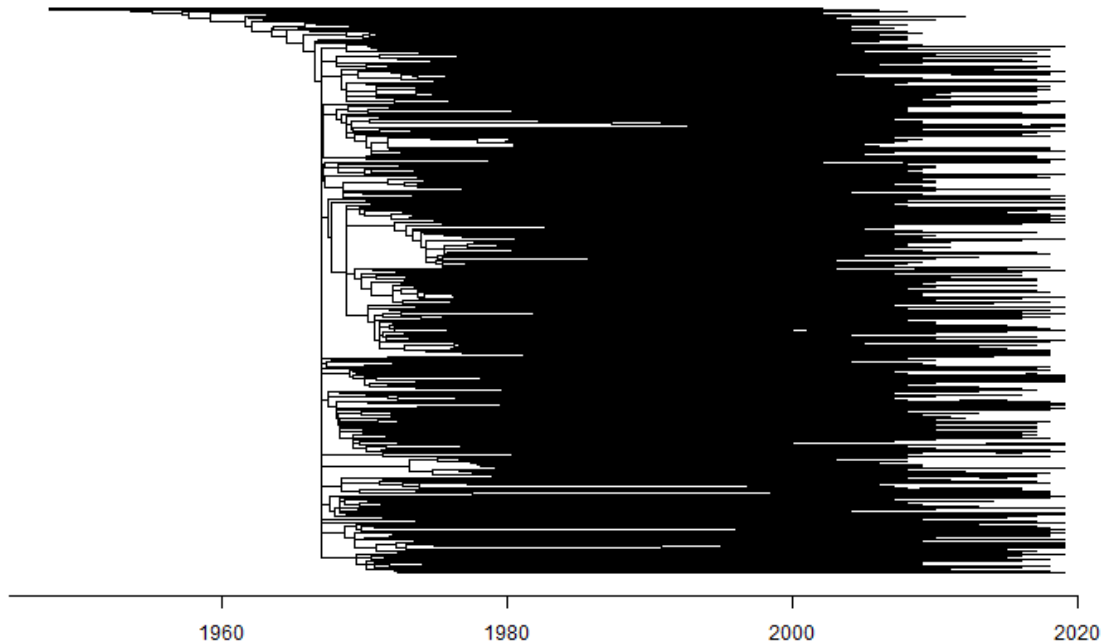


Figure 14: Dated phylogeny of HIV-1.

reporting probability is 76%. This is not surprising as it is estimated that 87% of people with HIV in the USA know that they have HIV (Disease Control and Prevention 2023). The posterior mean for X_0 is 2.3, which is close to the suspected initial value of 1. This suggests the the phylogenetic tree indeed reaches a most recent common ancestor when there were very few cases of HIV-1. The posterior mean for σ is 0.056, which is lower than the prior mean and initial value chosen of 0.1. This indicates that R_t is generally changing by at most ± 1.12 (i.e. ± 2 standard deviations) per year. The results of the inference of the latent prevalence are shown in Figure 17 and of R_t are shown in Figure 18.

Inference of the latent prevalence spans 1957 to 2019. We have only phylogenetic data from 1958 to 2009 and both phylogenetic and prevalence data from 2010 to 2019. The first cases of HIV-1 reported in the USA were in 1981, so it is difficult to draw conclusions for the accuracy of the prevalence inference prior to that. We can suppose that the prevalence of HIV-1 was low before 1981 to remain undiscovered. In 1981, the posterior mean of the inferred prevalence is 2,264 with a 95% credible interval of (1,228, 3,858). This is indeed low, although it should be noted that we only have data from North Carolina, so cannot generalise to the whole USA. The prevalence has an S-shape to it whereby cases increased slowly to around 1997, then rapidly to around 2008, and then slowly again to 2019. This may be because antiretroviral therapy was introduced in 1995, so more people were living with HIV-1 rather than dying from it, leading to a sharper increase in prevalence. A similar S-shaped prevalence trajectory can be seen in the National Institute on Drug Abuse’s HIV/AIDS Research Report (NIDA 2020).

Inference of the reproduction number spans 1958 to 2019. We have only phylogenetic data from 1958 to 2009 and both phylogenetic and prevalence data from 2010 to 2019. The inclusion of the epidemiological data to the phylogenetic data can be seen in the width of the credible interval. The mean width of the credible intervals from 1958 to 2009 is 3.6 and from 2010 to 2019 is 0.4. The combination of phylogenetic information and prevalence seems to provide a lot more certainty in

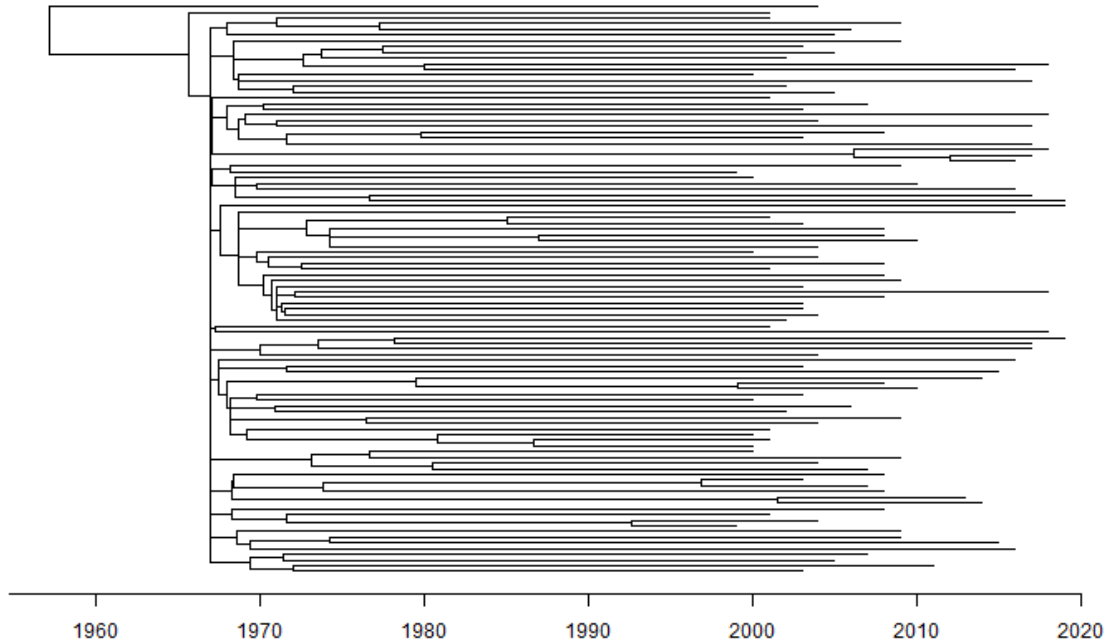


Figure 15: Sub-sample of the dated phylogeny of HIV-1.

the inference of the reproduction number compared with phylogenetic data alone. This is consistent with what we saw in the simulations, that the credible intervals using our method can be wide unless incorporating both sources of data.

The posterior mean in Figure 18 suggests that the effective reproduction number for HIV-1 in North Carolina has been above 1 since 1958. The posterior 2.5% quantile is above 1 from 1961 to 1981, from 2000 to 2001, and from 2012 to 2019, so we can be confident that HIV-1 was spreading during these times. Despite the width of the credible intervals, the phylogenetic data allows us to infer R_t with reasonable confidence much further back in time than the prevalence data.

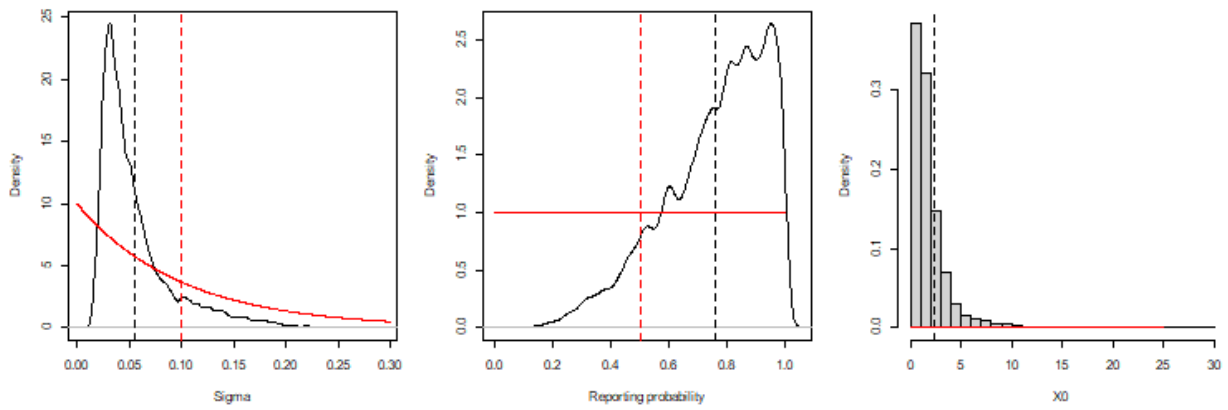


Figure 16: The posterior density of the reporting probability ρ is on the left, of σ is in the middle, and of X_0 is on the right in black. Priors are shown in red. The posterior mean is the dashed black vertical line and the prior mean is the dashed red vertical line.

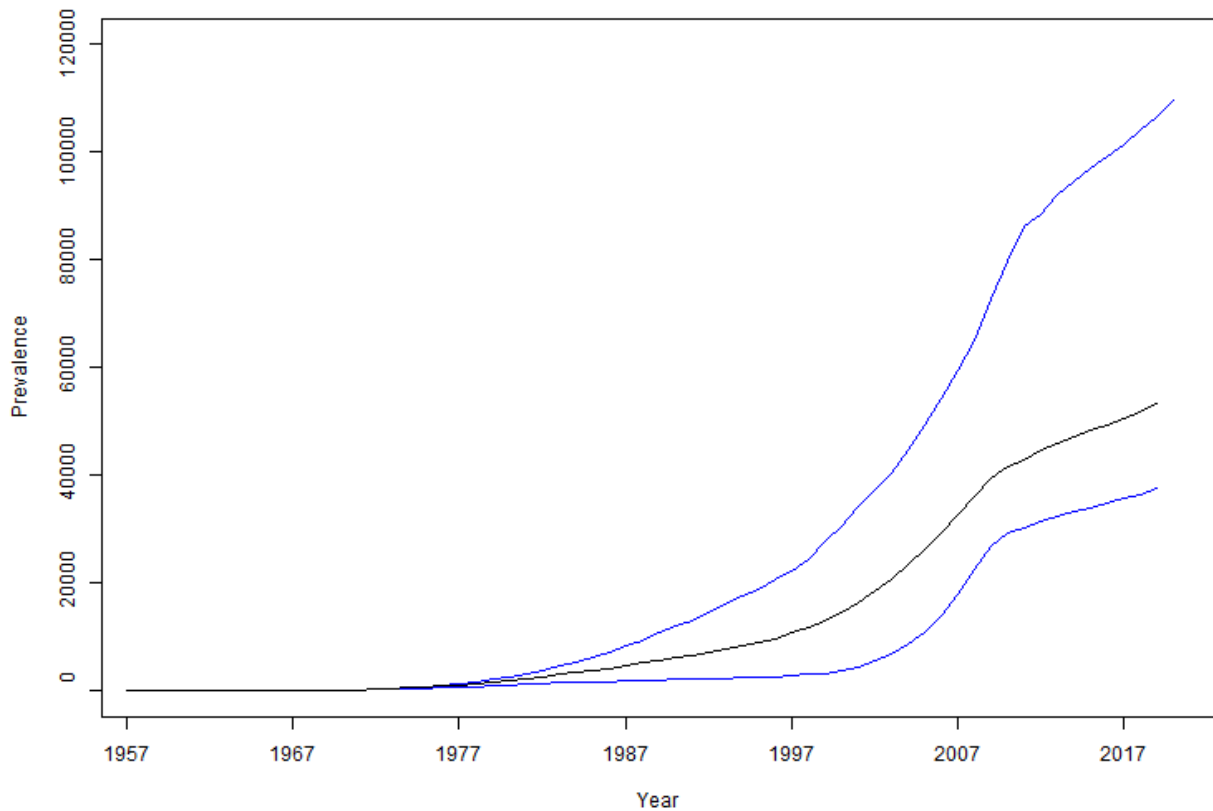


Figure 17: Inferred prevalence for the HIV-1 data set. The posterior mean is shown in black and the posterior 95% credible interval is shown in blue.

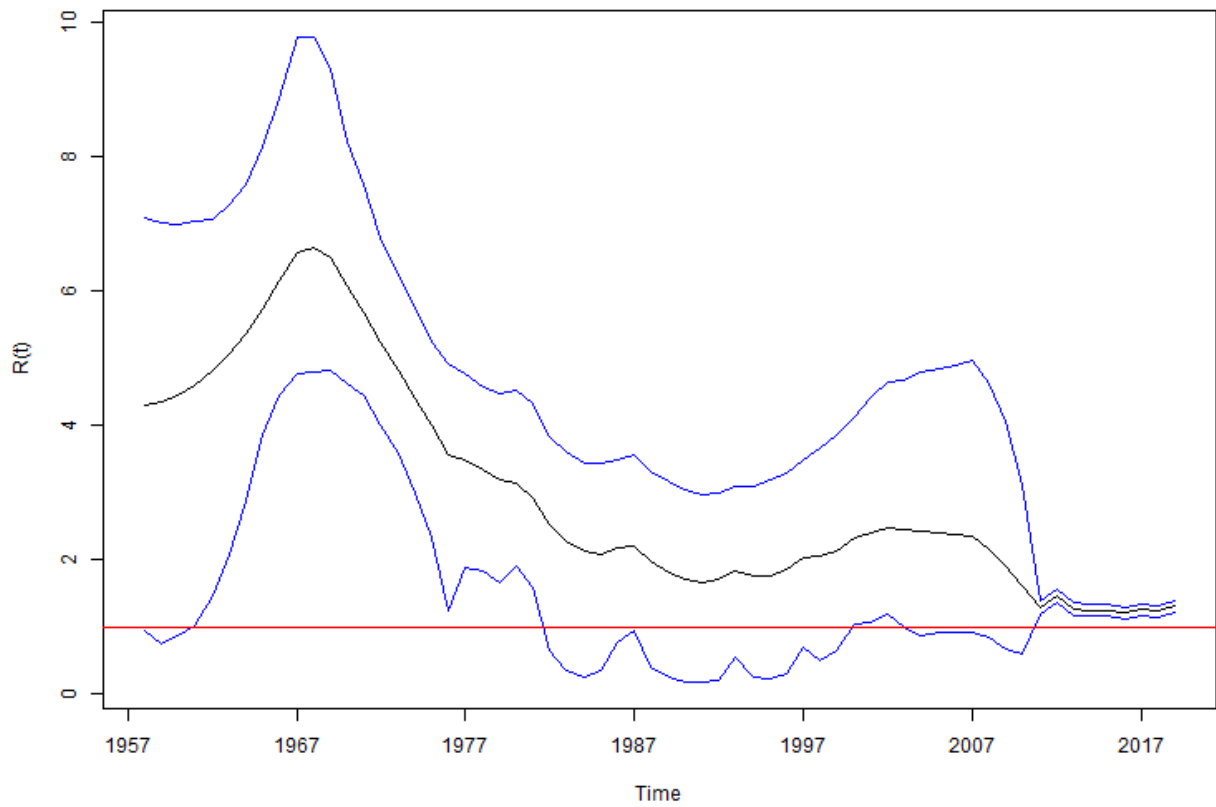


Figure 18: Inferred reproduction number for the HIV-1 data set. The posterior mean is shown in black and the posterior 95% credible interval is shown in blue. The red dashed line is $R_t = 1$ to make it clear when the posterior is above or below 1.

6 Discussion

6.1 Summary of findings

In this paper, we have introduced using particle MCMC methods, specifically the PMMH algorithm, to infer the reproduction number of an epidemic over time using a dated phylogeny and partially observed prevalence data.

In many simulated scenarios, the combination of data sources offers improvement in the inference and certainty of the inference in the reproduction number compared with one source or the other. In particular, the introduction of a small amount of epidemiological data to the genetic data drastically improves the inference. This is useful as in practice it is common to have a decent phylogenetic tree (as inference on phylogenetic trees is more robust to taking subtrees) and poor epidemiological information. Conversely, the introduction of genetic data to the epidemiological data vastly improves the inference of the reporting probability ρ .

We have also performed inference on a real data set. Inference in a real scenario is consistent with simulation results, in that inference of the reporting probability ρ is improved with combination data, as is certainty of R_t inference. We were able to compare the inferred latent prevalence to other sources to confirm that the inference seems to be giving accurate results. The real data inference also highlights that combination data allows for inference over a wider period of time than one source of data alone may allow.

6.2 Strengths and limitations

Whilst results look very promising, there are limitations to the approach. The epidemic model itself is rather simple. Compartment models are much more typical in epidemiology, such as susceptible-infectious-removed (SIR) or susceptible-exposed-infectious-recovered (SEIR) models. However, the simplicity of the model may not be an issue for inference when considering population-level data. Also, the reproduction number is still the ratio between β_t and γ_t in a SIR model, the most common epidemiological model, so the current birth-death model may still perform well in cases where an underlying SIR model would be more typically used. However, more work would be needed to extend the model to compartment models with more than 3 compartments, such as SEIR models or models with infectious people split by covariates. Our method would need to be tested on simulations of other underlying epidemic models and/or real data to examine its robustness to misspecification.

In practice, the dated phylogeny would be estimated using sequencing data, and this paper does not address the uncertainty inherent in the dated phylogeny. However, methods such as BEAST and BEAST2 generate posterior phylogenies given sequencing data using MCMC, so we could incorporate this uncertainty by running our method on more than one replicate of the phylogeny output from BEAST/BEAST2. We can also see from our simulations that the inference from the genetic trees does not vary much as we change the size of the tree, so we may expect that the additional uncertainty will be fairly small.

Addressing these limitations and thus extending the method to a wider range of applications forms the basis for future work.

Acknowledgements

Alicia Gill was supported by EPSRC grant EP/R513374/1. Jere Koskela was supported by EPSRC research grant EP/V049208/1. Xavier Didelot received funding from the NIHR Health Protection Research Unit in Genomics and Enabling Data. Richard G. Everitt was supported by EPSRC grant EP/W006790/1 and NERC grant NE/T00973X/1.

References

- Andrieu, Christophe, Doucet, Arnaud, and Holenstein, Roman (2010). “Particle Markov chain Monte Carlo methods”. In: *Journal of the Royal Statistical Society Series B* 72.3, pp. 269–342. DOI: 10.1111/j.1467-9868.2009.00736.x.
- Andrieu, Christophe and Roberts, Gareth O. (2009). “The pseudo-marginal approach for efficient Monte Carlo computations”. In: *Annals of Statistics* 37.2, pp. 697–725. DOI: 10.1214/07-AOS574.
- Boonpatcharanon, Sawitree, Hefferman, Jane, and Jankowski, Hannah (2022). “Estimating the basic reproduction number at the beginning of an outbreak”. In: *PLOS ONE* 17.6. DOI: 10.1371/journal.pone.0269306.
- Bouckaert, Remco et al. (2019). “BEAST 2.5: An advanced software platform for Bayesian evolutionary analysis”. In: *PLoS Computational Biology* 15.4, e1006650. DOI: 10.1371/journal.pcbi.1006650.
- Chopin, Nicolas and Papaspiliopoulos, Omiros (2020). *An Introduction to Sequential Monte Carlo*. Springer Series in Statistics. Springer Cham. ISBN: 978-3-030-47845-2. DOI: 10.1007/978-3-030-47845-2.
- Cori, Anne et al. (2013). “A New Framework and Software to Estimate Time-Varying Reproduction Numbers during Epidemics”. In: *American Journal of Epidemiology* 178.9, pp. 1505–1512. DOI: 10.1093/aje/kwt133..
- Didelot, Xavier and Parkhill, Julian (2022). “A scalable analytical approach from bacterial genomes to epidemiology”. In: *Philosophical Transactions of the Royal Society B: Biological Sciences* 377.1861, p. 20210246. DOI: 10.1098/rstb.2021.0246.
- Didelot, Xavier et al. (2018). “Bayesian inference of ancestral dates on bacterial phylogenetic trees”. In: *Nucleic Acids Research* 46.22, e134. DOI: 10.1093/nar/gky783.
- Didelot, Xavier et al. (2023). “Model design for nonparametric phylodynamic inference and applications to pathogen surveillance”. In: *Virus Evolution* 9.1, vead028. DOI: 10.1093/ve/vead028.
- Disease Control, Centers for and Prevention (2023). *Estimated HIV incidence and prevalence in the United States, 2017–2021*. URL: <https://www.cdc.gov/hiv/library/reports/hiv-surveillance/vol-28-no-3/index.html>. (accessed: 04.11.2023).
- Doucet, Arnaud and Johansen, Adam (2011). “A Tutorial on Particle Filtering and Smoothing: Fifteen years later”. In: *The Oxford Handbook of Nonlinear Filtering*. Ed. by Dan Crisan and Boris Rozovskii. Oxford University Press. Chap. 24.
- Drummond, Alexei J. et al. (2002). “Estimating Mutation Parameters, Population History and Genealogy Simultaneously From Temporally Spaced Sequence Data”. In: *Genetics* 161.3, pp. 1307–1320. DOI: 10.1093/genetics/161.3.1307.
- Dyk, David A. van and Meng, Xiao-Li (2001). “The Art of Data Augmentation”. In: *Journal of Computational and Graphical Statistics* 10.1, pp. 1–50. DOI: 10.1198/10618600152418584.
- Frost, Simon D. W. and Volz, Erik (2010). “Viral phylodynamics and the search for an ‘effective number of infections’”. In: *Philosophical transactions of the Royal Society of London. Series B, Biological sciences* 365.1548, pp. 1879–1890. DOI: 10.1098/rstb.2010.0060.
- Gamado, Kokouvi M., Streftaris, George, and Zachary, Stan (2014). “Modelling under-reporting in epidemics”. In: *Journal of Mathematical Biology* 69, pp. 737–765. DOI: 10.1007/s00285-013-0717-z.
- (2017). “Estimation of under-reporting in epidemics using approximations”. In: *Journal of Mathematical Biology* 74, pp. 1683–1707. DOI: 10.1007/s00285-016-1064-7.
- Godshill, Simon J., Doucet, Arnaud, and West, Mike (2004). “Monte Carlo Smoothing for Nonlinear Time Series”. In: *Journal of the American Statistical Association* 99.465, pp. 156–168. DOI: 10.1198/016214504000000151.
- Hastings, W.K. (1970). “Monte Carlo sampling methods using Markov chains and their applications”. In: *Biometrika* 57.1, pp. 97–109. DOI: 10.1093/biomet/57.1.97.

- Ho, Simon Y. W. and Shapiro, Beth (2011). “Skyline-plot methods for estimating demographic history from nucleotide sequences”. In: *Molecular Ecology Resources* 11.3, pp. 423–434. DOI: 10.1111/j.1755-0998.2011.02988.x.
- Karcher, Michael D. et al. (2017). “phylodyn: an R package for phylodynamic simulation and inference”. In: *Molecular ecology resources* 17.1, pp. 96–100. DOI: 10.1111/1755-0998.12630.
- Kendall, David (1948). “On the generalized “birth-and-death” process”. In: *Annals of Mathematical Statistics* 19.1, pp. 1–15. DOI: 10.1214/aoms/1177730285.
- Kingman, J. F. C. (1982). “The coalescent”. In: *Stochastic Processes and their Applications* 13.3, pp. 235–248. DOI: 10.1016/0304-4149(82)90011-4.
- Koelle, Katia and Rasmussen, David A. (2012). “Rates of coalescence for common epidemiological models at equilibrium”. In: *Journal of The Royal Society Interface* 9, pp. 997–1007. DOI: 10.1098/rsif.2011.0495.
- Lash, Timothy L. et al. (2021). *Modern Epidemiology*. 4th ed. Philadelphia, PA: Wolters Kluwer. ISBN: 9781975166281.
- Leone, F. C., Nelson, L. S., and Nottingham, R. B. (1961). “The Folded Normal Distribution”. In: *Technometrics* 2.4, pp. 543–550. DOI: 10.1080/00401706.1961.10489974.
- Liang, Wei, Dai, Hongsheng, and Restaino, Marialuisa (2022). “Truncation data analysis for the under-reporting probability in COVID-19 pandemic”. In: *Journal of Nonparametric Statistics* 34.3, pp. 607–627. DOI: 10.1080/10485252.2021.1989426.
- NIDA (2020). *How Does Drug Abuse Affect the HIV Epidemic?* URL: <https://nida.nih.gov/publications/research-reports/hivaids/how-does-drug-abuse-affect-hiv-epidemic>. (Accessed: 13/11/2023).
- Pitt, Michael K. et al. (2012). “On some properties of Markov chain Monte Carlo simulation methods based on the particle filter”. In: *Journal of Econometrics* 171.2, pp. 134–151. DOI: 10.1016/j.jeconom.2012.06.004.
- Rasmussen, David A., Ratmann, Oliver, and Koelle, Katia (2011). “Inference for Nonlinear Epidemiological Models Using Genealogies and Time Series”. In: *PLOS Computational Biology* 7.8, e1002136. DOI: 10.1371/journal.pcbi.1002136.
- Sagulenko, Pavel, Puller, Vadim, and Neher, Richard A. (2018). “TreeTime: Maximum-likelihood phylodynamic analysis”. In: *Virus Evolution* 4.1, vex042. DOI: 10.1093/ve/vex042.
- Sherlock, Chris et al. (2015). “On the Efficiency of Pseudo-Marginal Random Walk Metropolis Algorithms”. In: *The Annals of Statistics* 43.1, pp. 23–275. DOI: 10.1214/14-AOS1278.
- Skellam, J. G. (1946). “The Frequency Distribution of the Difference Between Two Poisson Variates Belonging to Different Populations”. In: *Journal of the Royal Statistical Society* 109.3, p. 296. DOI: 10.2307/2981372.
- Stadler, Tanja (2009). “On incomplete sampling under birth–death models and connections to the sampling-based coalescent”. In: *Journal of Theoretical Biology* 261.1, pp. 58–66. DOI: 10.1016/j.jtbi.2009.07.018.
- (2010). “Sampling-through-time in birth–death trees”. In: *Journal of Theoretical Biology* 267.3, pp. 396–404. DOI: 10.1016/j.jtbi.2010.09.010.
- Stoner, Oliver, Economou, Theo, and Drummond Marques da Silva, Gabriela (2019). “A Hierarchical Framework for Correcting Under-Reporting in Count Data”. In: *Journal of the American Statistical Association* 114.528, pp. 1481–1492. DOI: 10.1080/01621459.2019.1573732.
- Suchard, Marc A et al. (2018). “Bayesian Phylogenetic and Phylodynamic Data Integration Using BEAST 1.10”. In: *Virus Evolution* 4.1, vey016. DOI: /10.1093/ve/vey016.
- To, Thu-Hien et al. (2016). “Fast Dating Using Least-Squares Criteria and Algorithms”. In: *Systematic Biology* 65.1, pp. 82–97. DOI: 10.1093/sysbio/syv068.
- Vaughan, Timothy G. et al. (2019). “Estimating Epidemic Incidence and Prevalence from Genomic Data”. In: *Molecular Biology and Evolution* 36.8, pp. 1804–1816. DOI: 10.1093/molbev/msz106.
- Vihola, Matti (2011). “On the stability and ergodicity of adaptive scaling Metropolis algorithms”. In: *Stochastic Processes and their Applications* 121.12, pp. 2839–2860. DOI: 10.1016/j.spa.2011.08.006.

- Volz, Erik (2012). “Complex Population Dynamics and the Coalescent Under Neutrality”. In: *Genetics* 191.1, pp. 187–201. DOI: 10.1534/genetics.111.134627.
- Volz, Erik and Didelot, Xavier (2018). “Modeling the Growth and Decline of Pathogen Effective Population Size Provides Insight into Epidemic Dynamics and Drivers of Antimicrobial Resistance”. In: *Systematic Biology* 67.4, pp. 719/728. DOI: 10.1093/sysbio/syy007.
- Volz, Erik and Frost, Simon D. W. (2014). “Sampling through time and phylodynamic inference with coalescent and birth–death models”. In: *Journal of the Royal Society Interface* 11.101, p. 20140945. DOI: 10.1098/rsif.2014.0945.
- (2017). “Scalable relaxed clock phylogenetic dating”. In: *Virus Evolution* 3.2, vex025. DOI: 10.1093/ve/vex025.
- Volz, Erik et al. (2009). “Phylodynamics of infectious disease epidemics”. In: *Genetics* 183.4, pp. 1421–1430. DOI: 10.1534/genetics.109.106021.
- Wallinga, Jacco and Teunis, Peter (2004). “Different epidemic curves for severe acute respiratory syndrome reveal similar impacts of control measures”. In: *American Journal of Epidemiology* 160.6, pp. 509–516. DOI: 10.1093/aje/kwh255.

A Appendix - Reducing path degeneracy

To demonstrate empirically the improvements from implementing systematic resampling, adaptive resampling and backward simulation, we have run some simulations which can be seen in Figure 19. In these simulations, the true birth rate is constant at 0.3, so σ should be close to 0. We suppose that 5% of the true prevalence has been observed, so the true ρ is 0.05. We have run the SMC algorithm 100 times with $\sigma = 0.01$, $\rho = 0.05$ and $K = 1000$, and for each run output a sample trajectory of the birth rate. On the left are the 100 birth rate trajectories with multinomial resampling, resampling in every step and no backward simulation. On the right are the 100 birth rate trajectories with systematic resampling, only resampling if the ESS falls below $K/2$ and backward simulation.

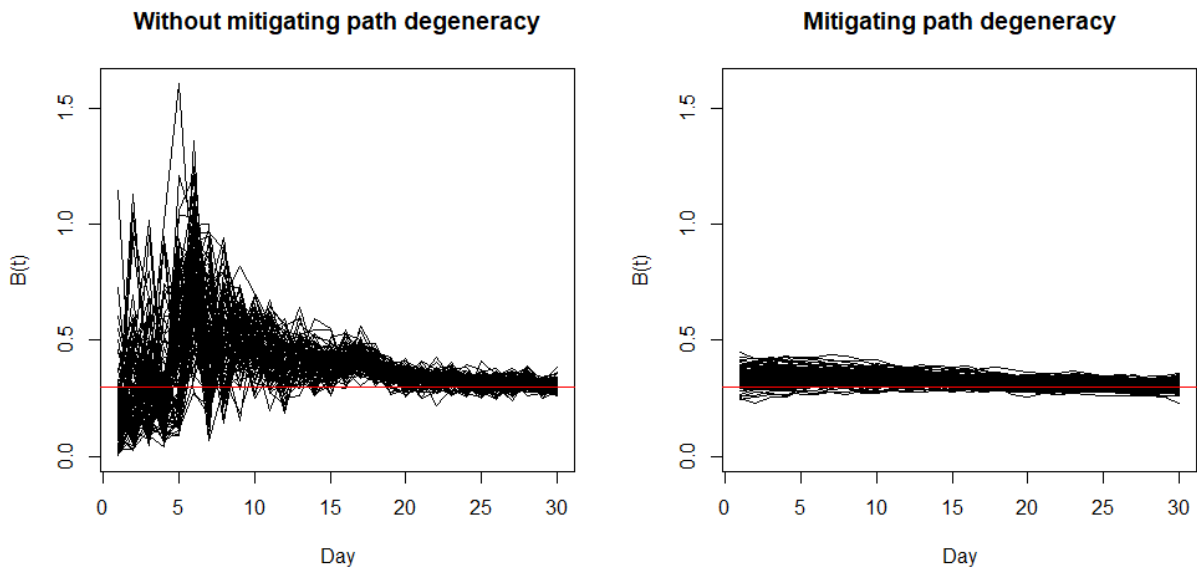


Figure 19: Comparison of birth rate inference with and without methods to reduce path degeneracy.

B Appendix - Performance diagnostics

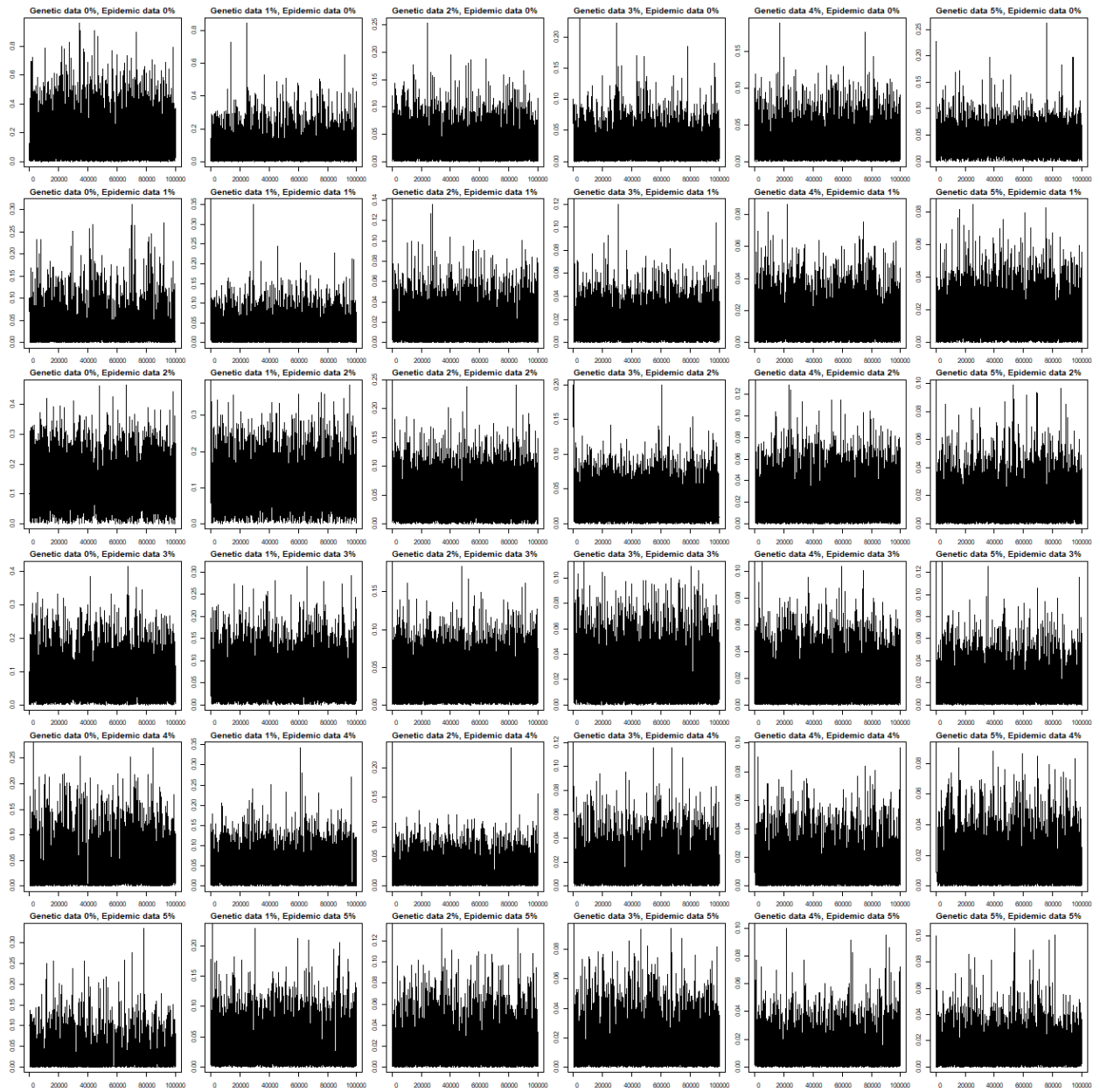


Figure 20: Trace plots for σ for a simulated epidemic with a constant birth rate.

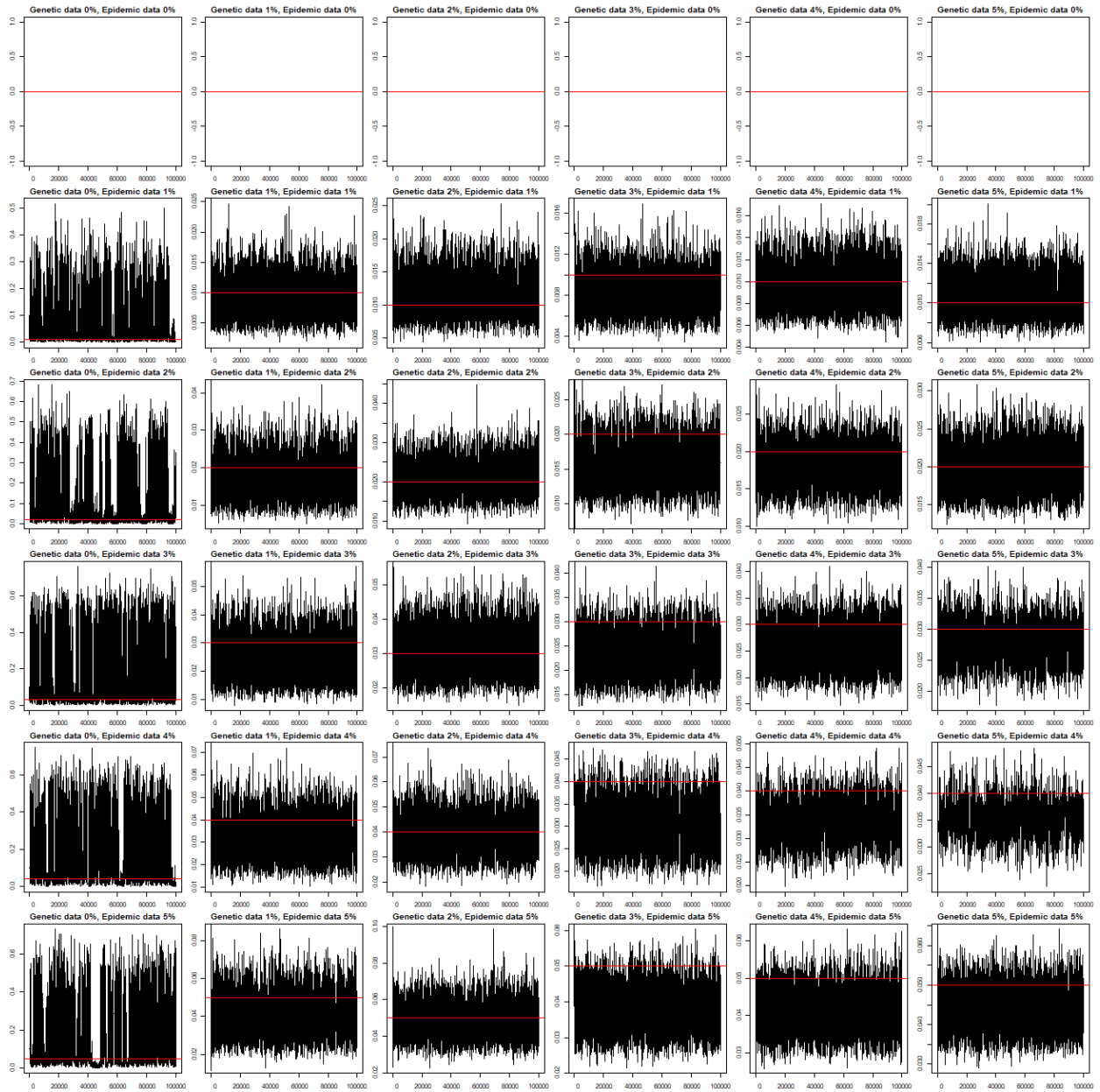


Figure 21: Trace plots for ρ for a simulated epidemic with a constant birth rate. The red line denotes the true value of the parameter ρ .

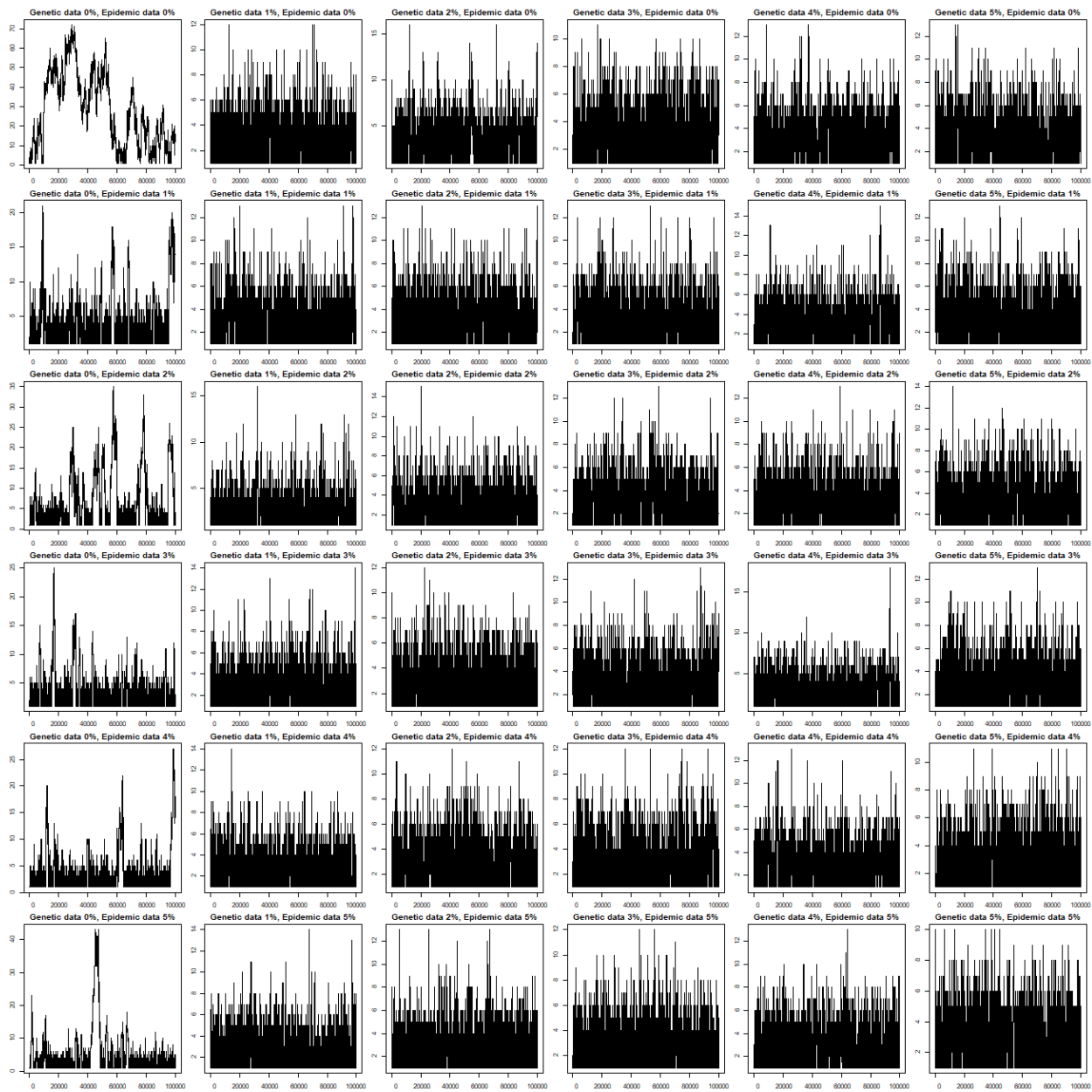


Figure 22: Trace plots for X_0 for a simulated epidemic with a constant birth rate.

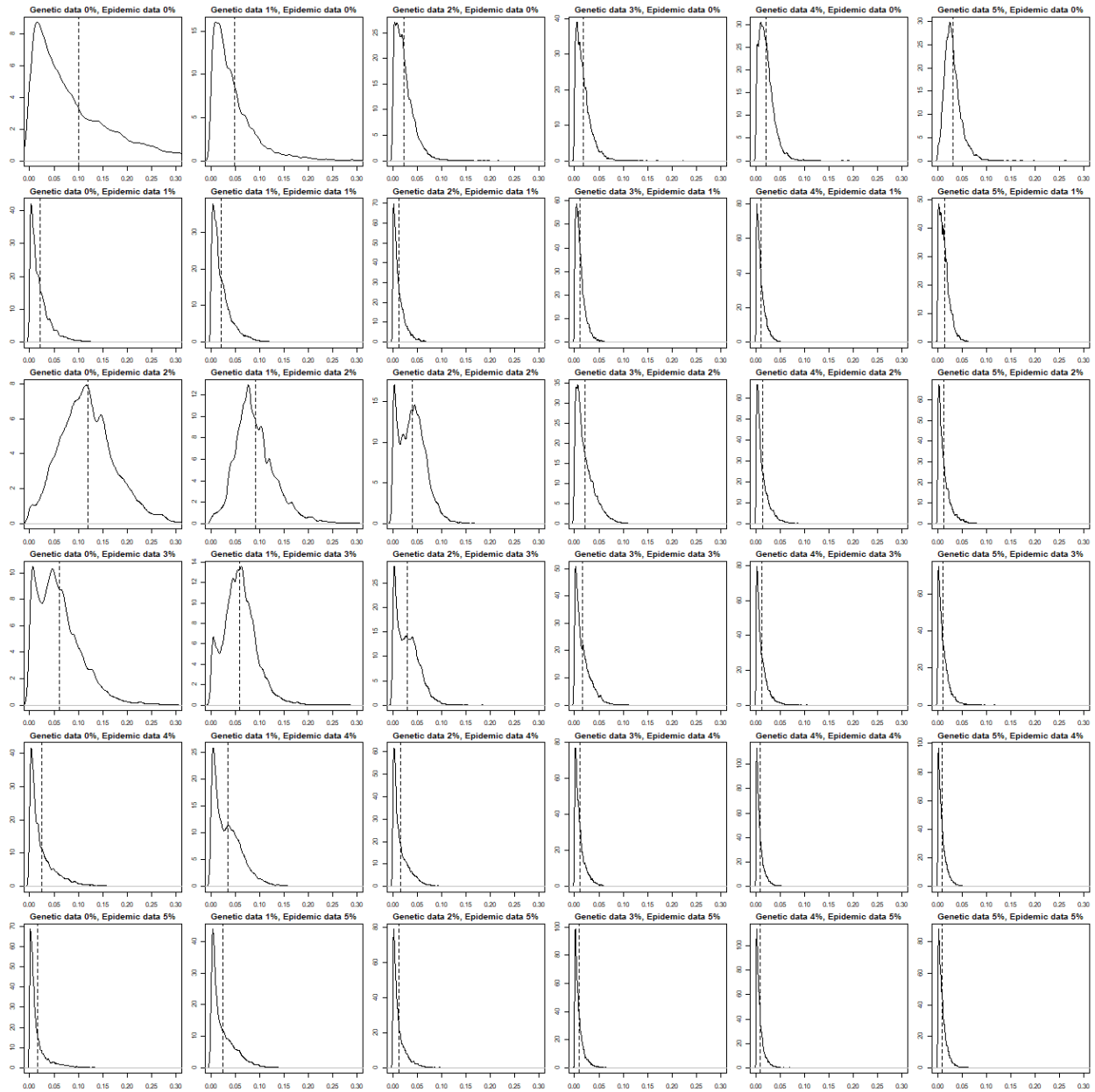


Figure 23: Posterior density of σ for a simulated epidemic with a constant birth rate. The dashed black line represents the posterior mean.

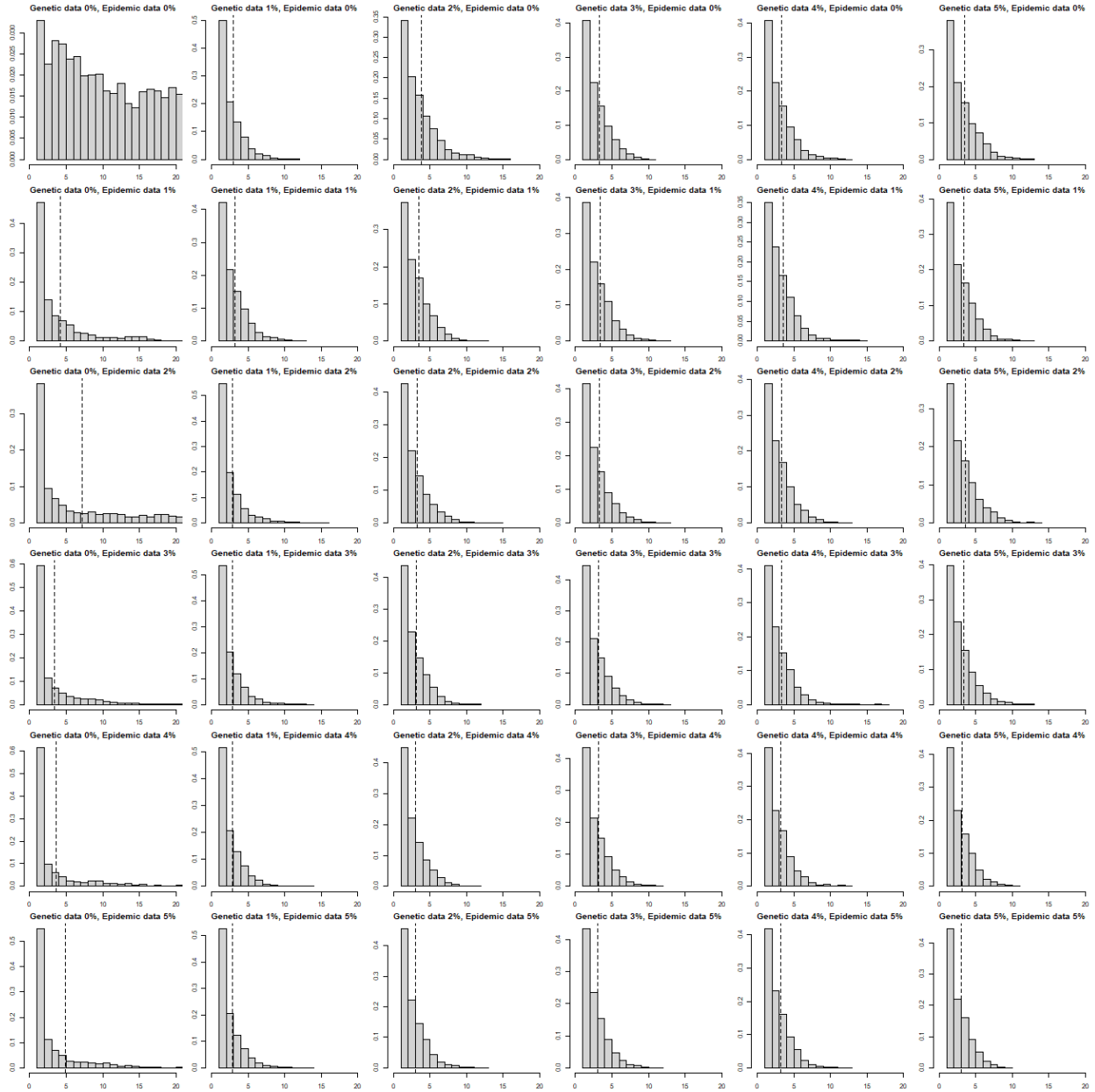


Figure 24: Posterior density histogram of the number of cases on day 0 for a simulated epidemic with a constant birth rate. The dashed black line represents the posterior mean.

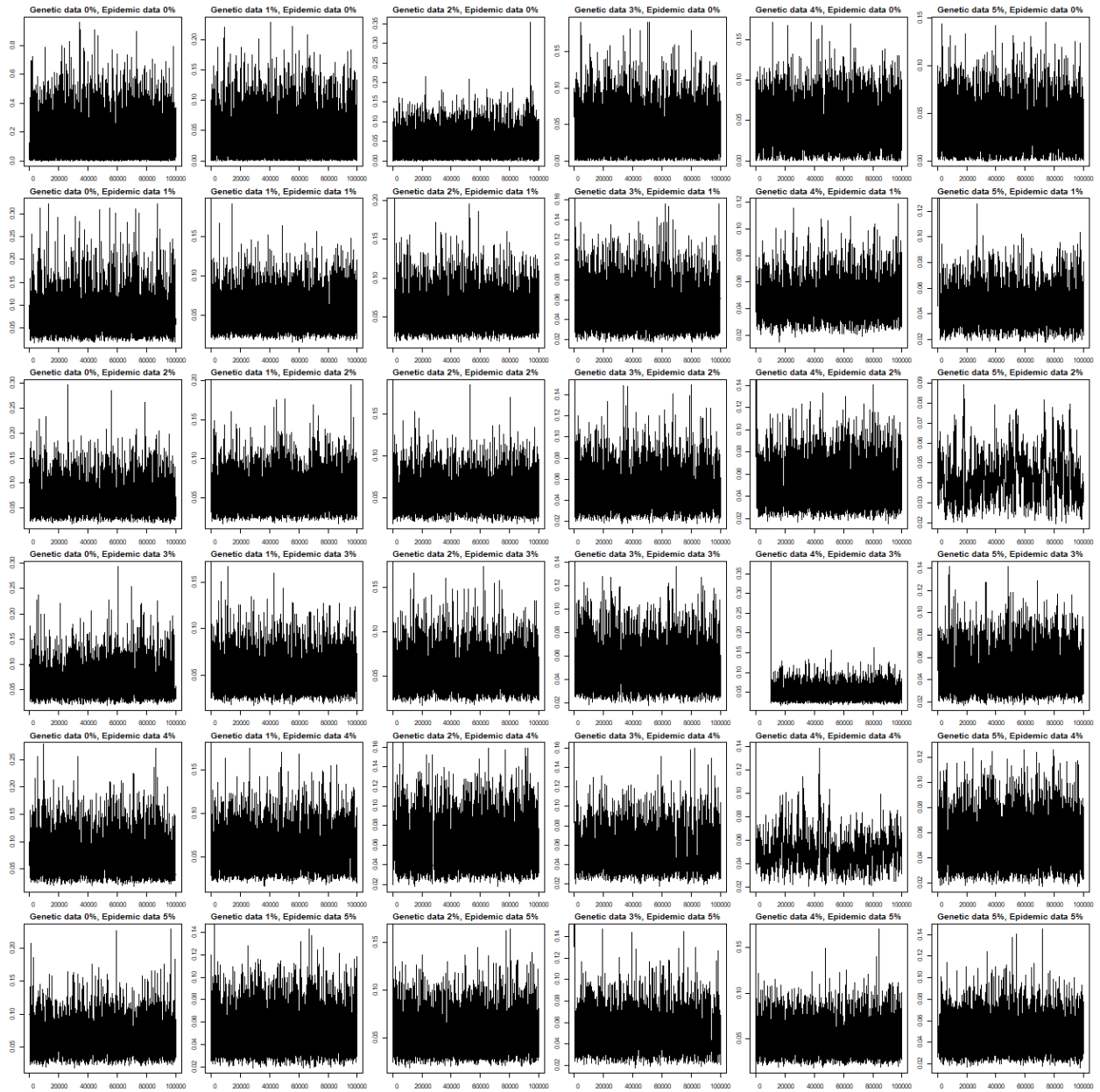


Figure 25: Trace plots for σ for a simulated epidemic with a peaked birth rate.

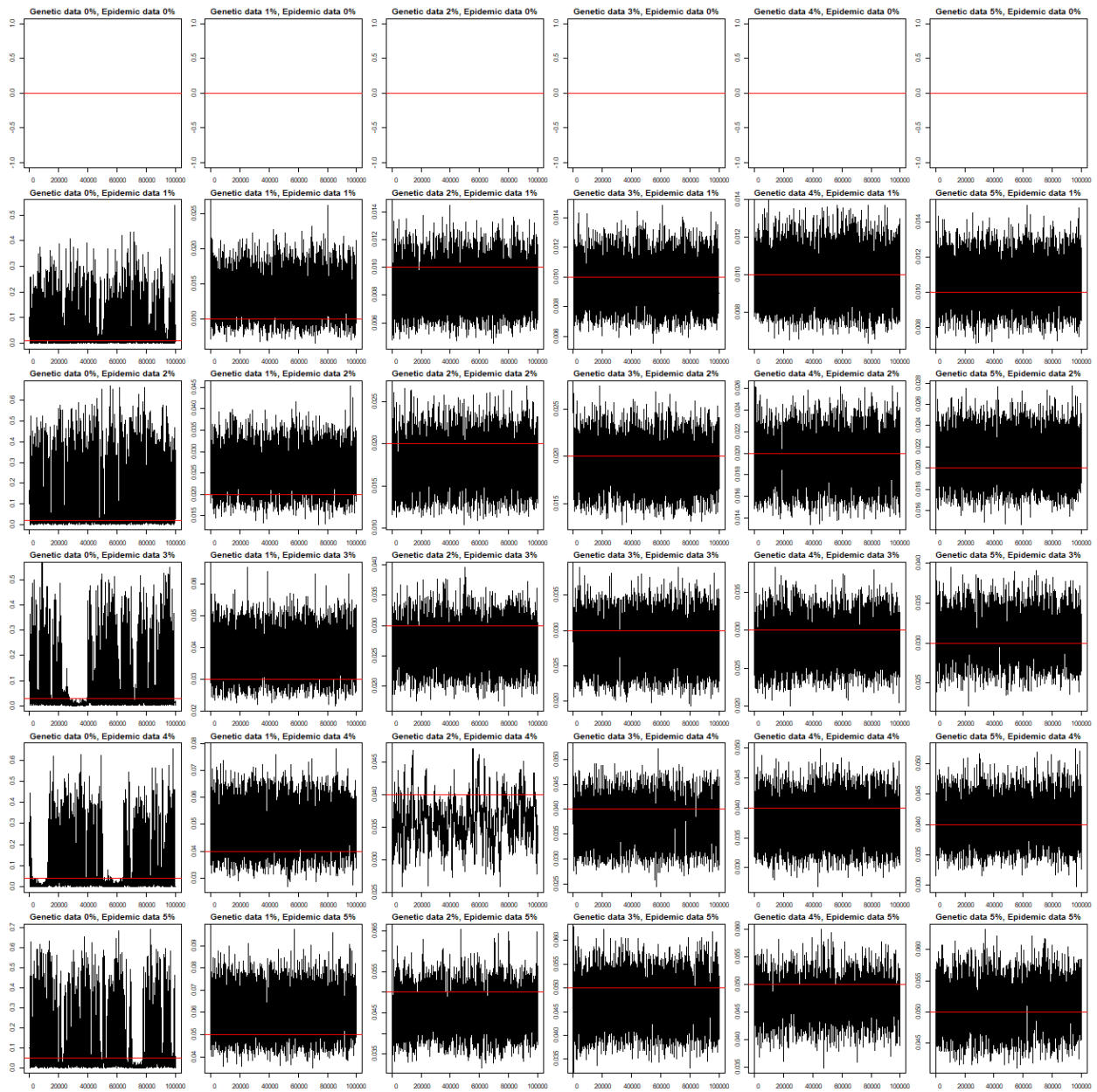


Figure 26: Trace plots for ρ for a simulated epidemic with a peaked birth rate. The red line denotes the true value of the parameter ρ .

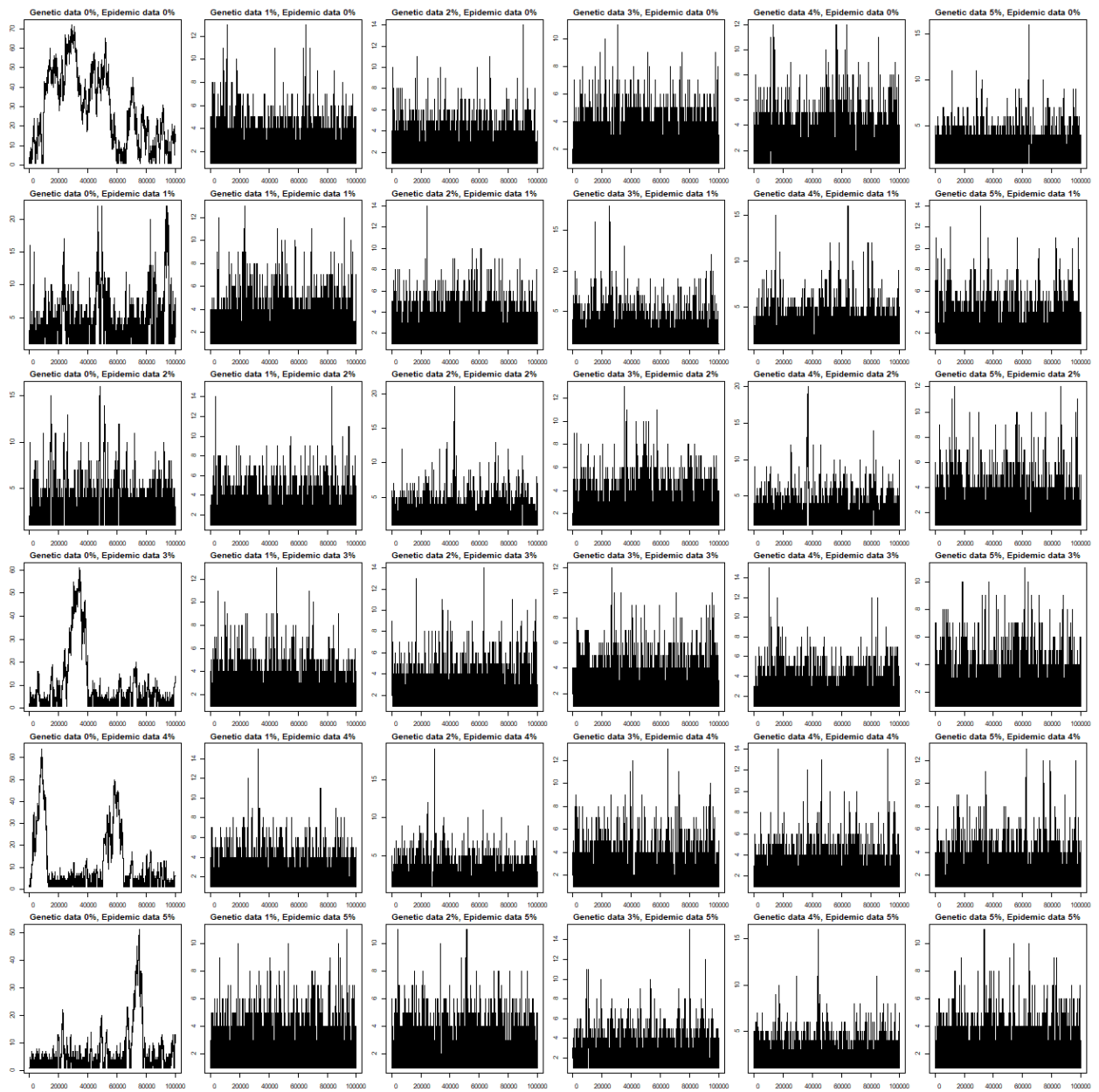


Figure 27: Trace plots for X_0 for a simulated epidemic with a peaked birth rate.

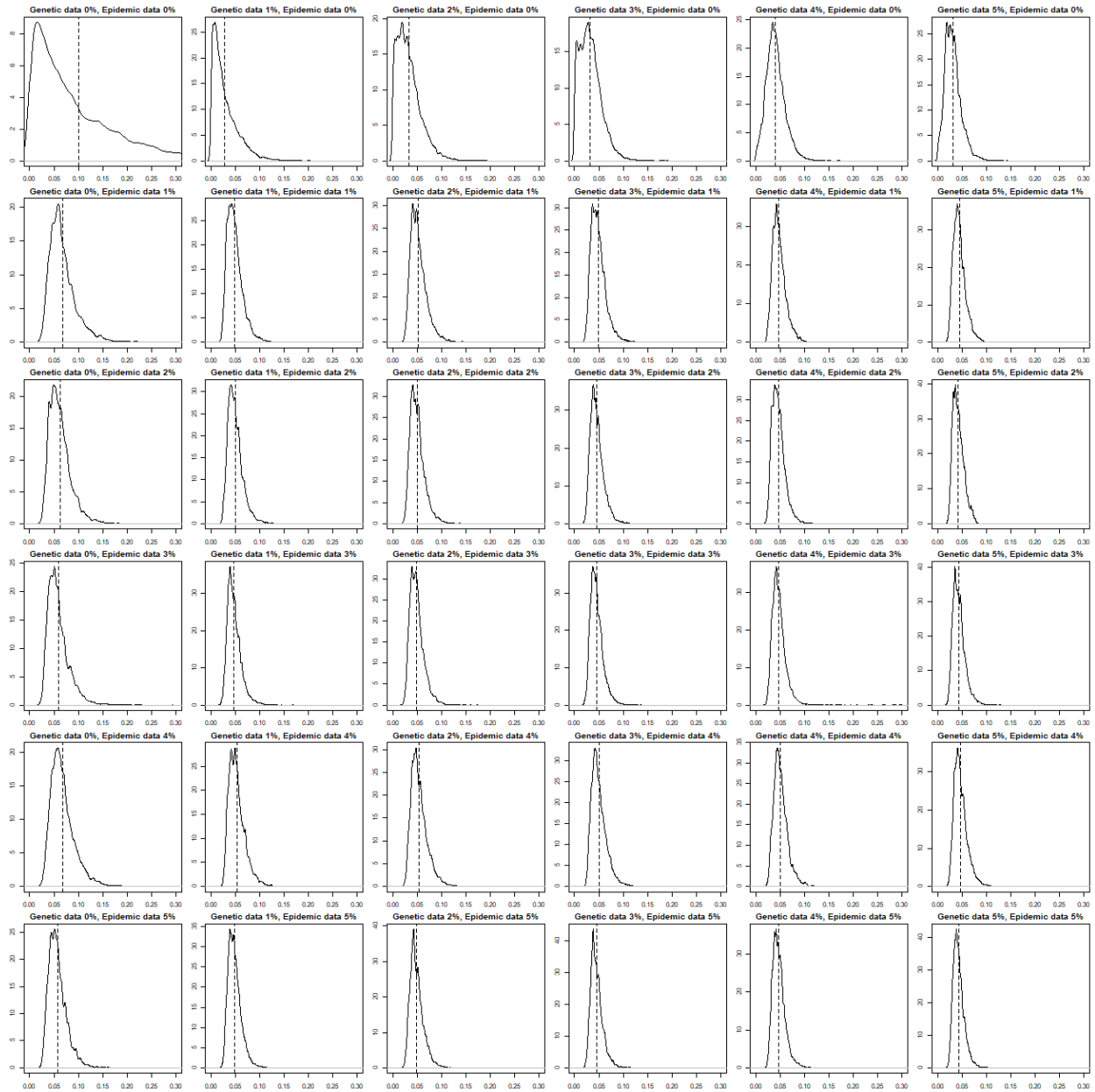


Figure 28: Posterior density of σ for a simulated epidemic with a peaked birth rate. The dashed black line represents the posterior mean.

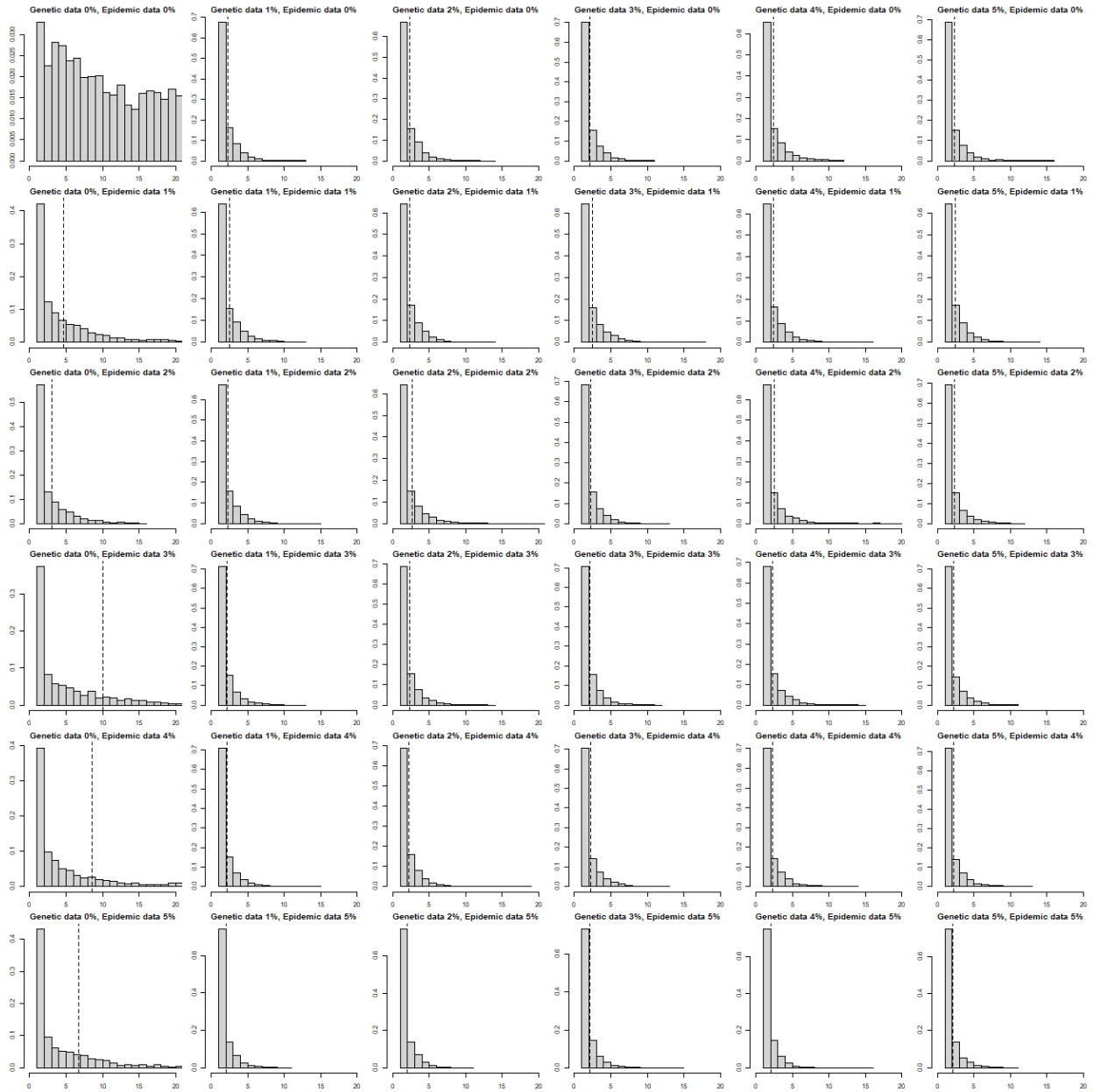


Figure 29: Posterior density histogram of the number of cases on day 0 for a simulated epidemic with a peaked birth rate. The dashed black line represents the posterior mean.

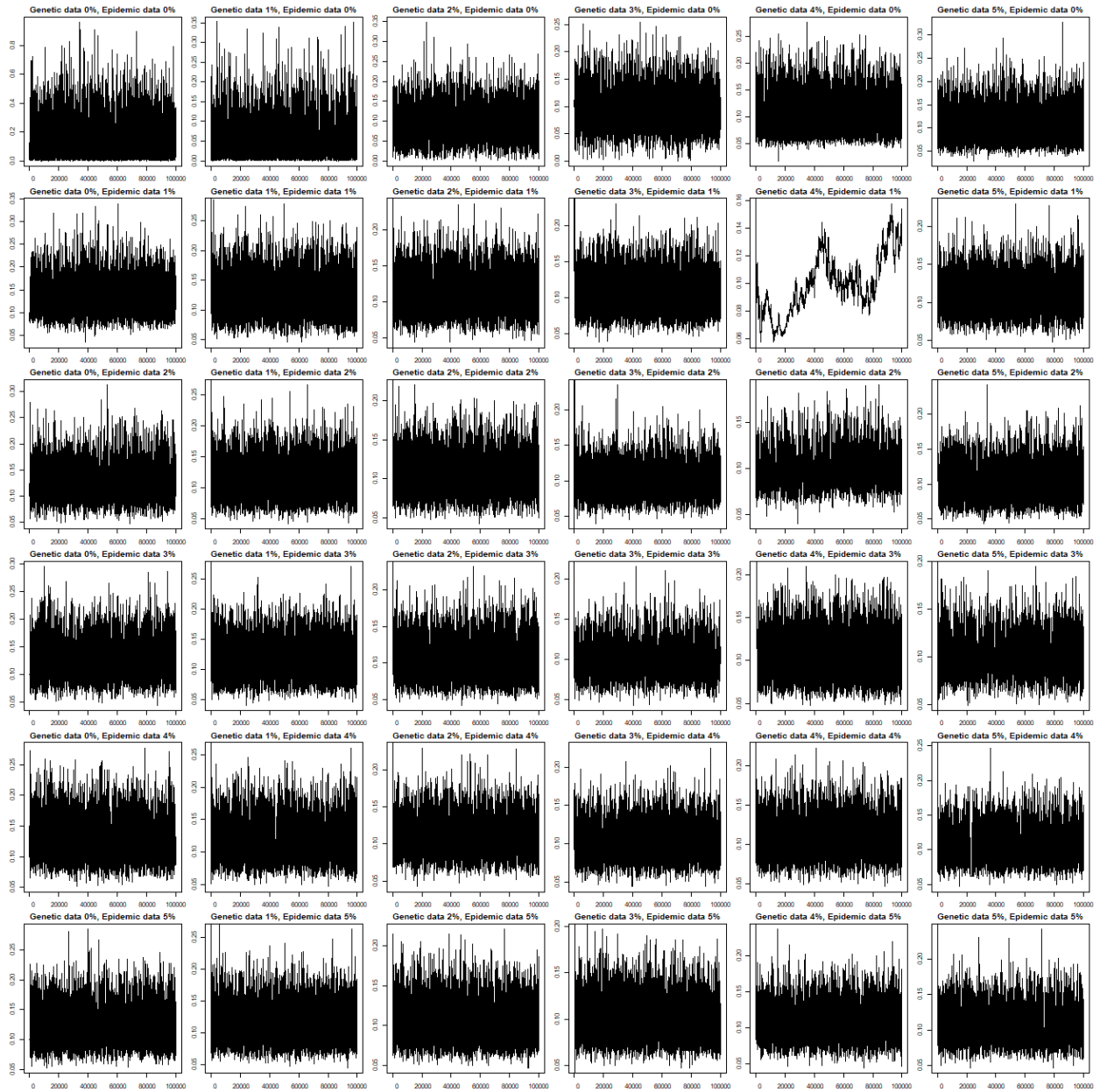


Figure 30: Trace plots for σ for a simulated epidemic with a change point birth rate.

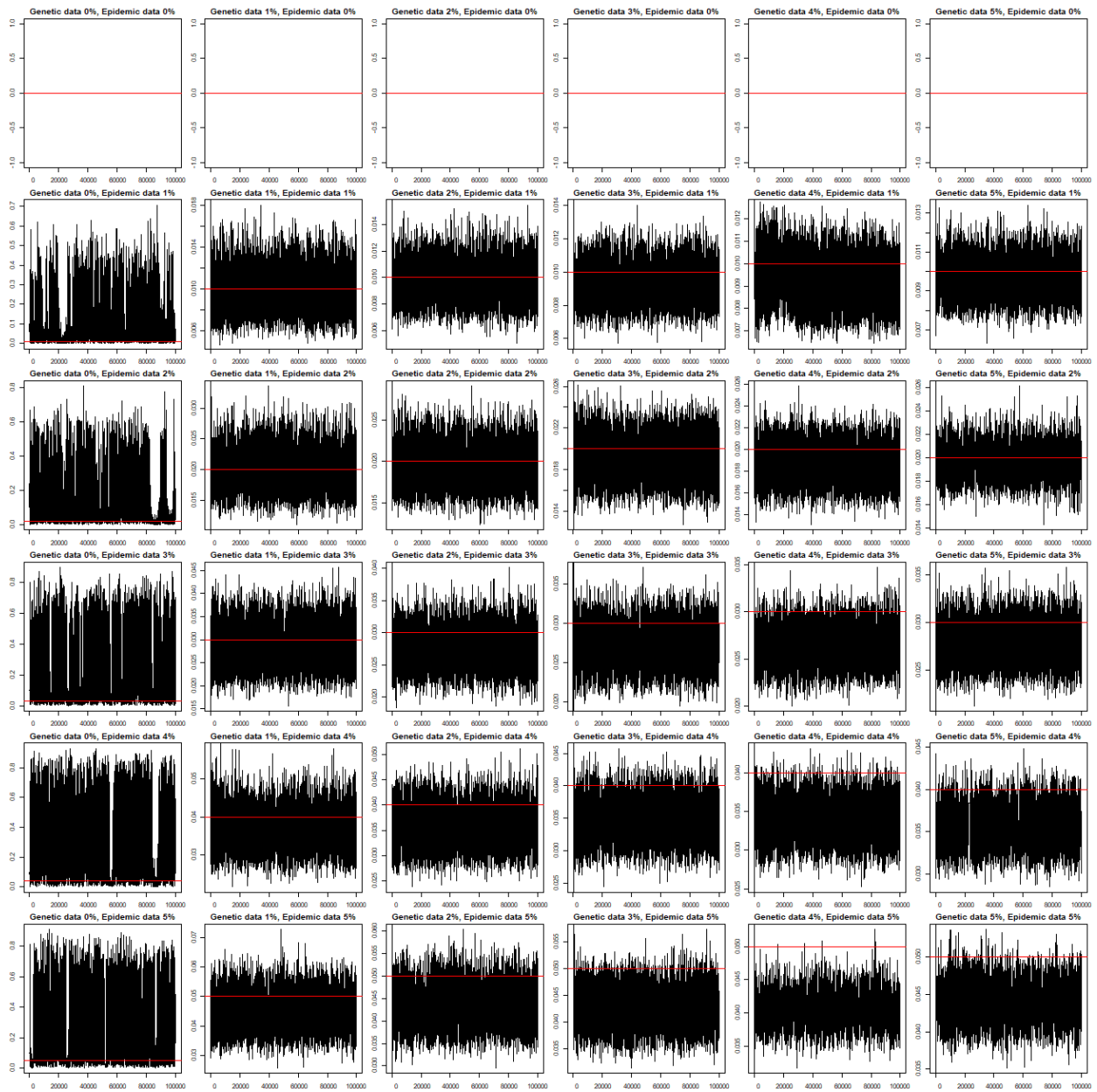


Figure 31: Trace plots for ρ for a simulated epidemic with a change point birth rate. The red line denotes the true value of the parameter ρ .

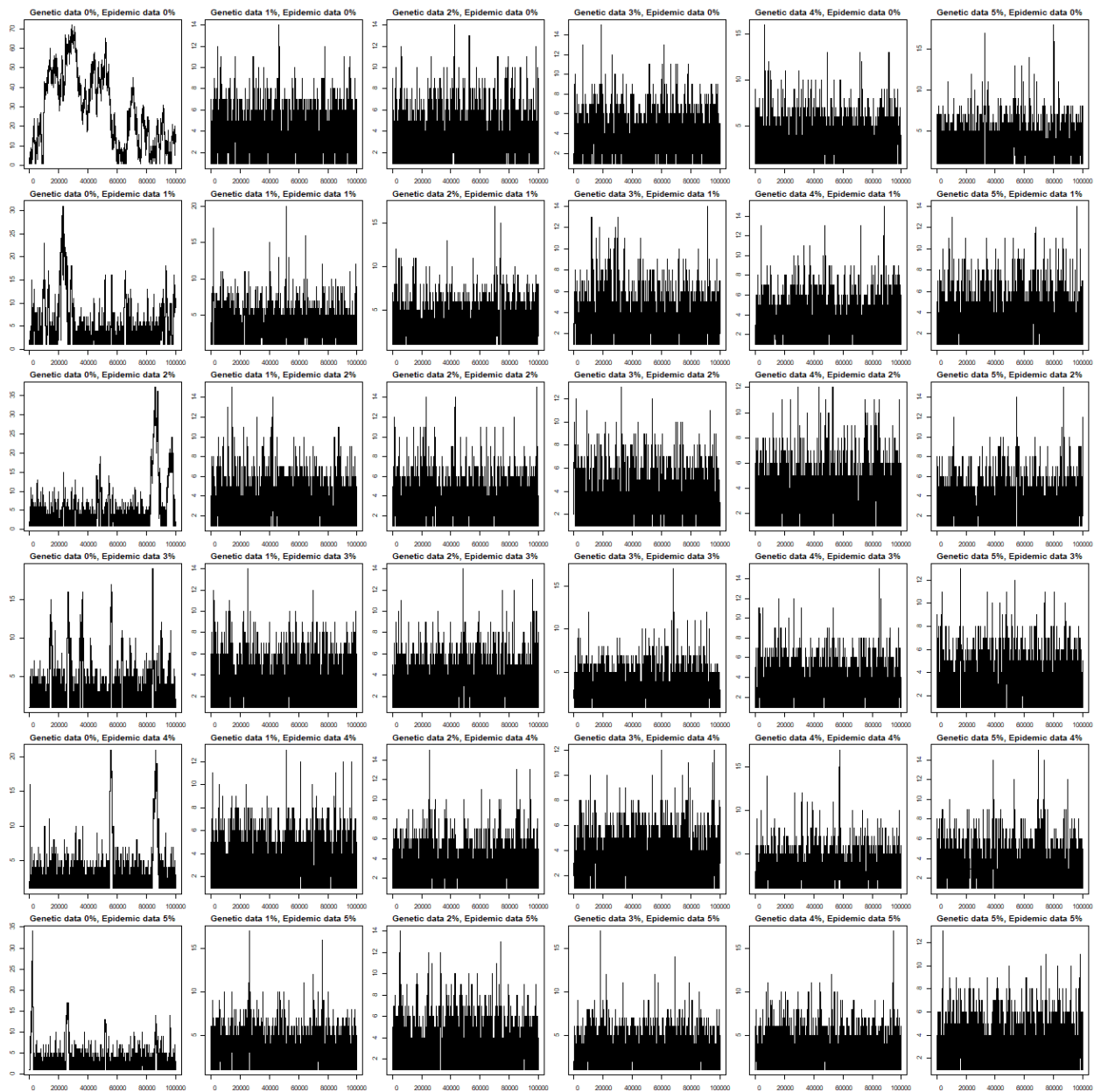


Figure 32: Trace plots for X_0 for a simulated epidemic with a change point birth rate.

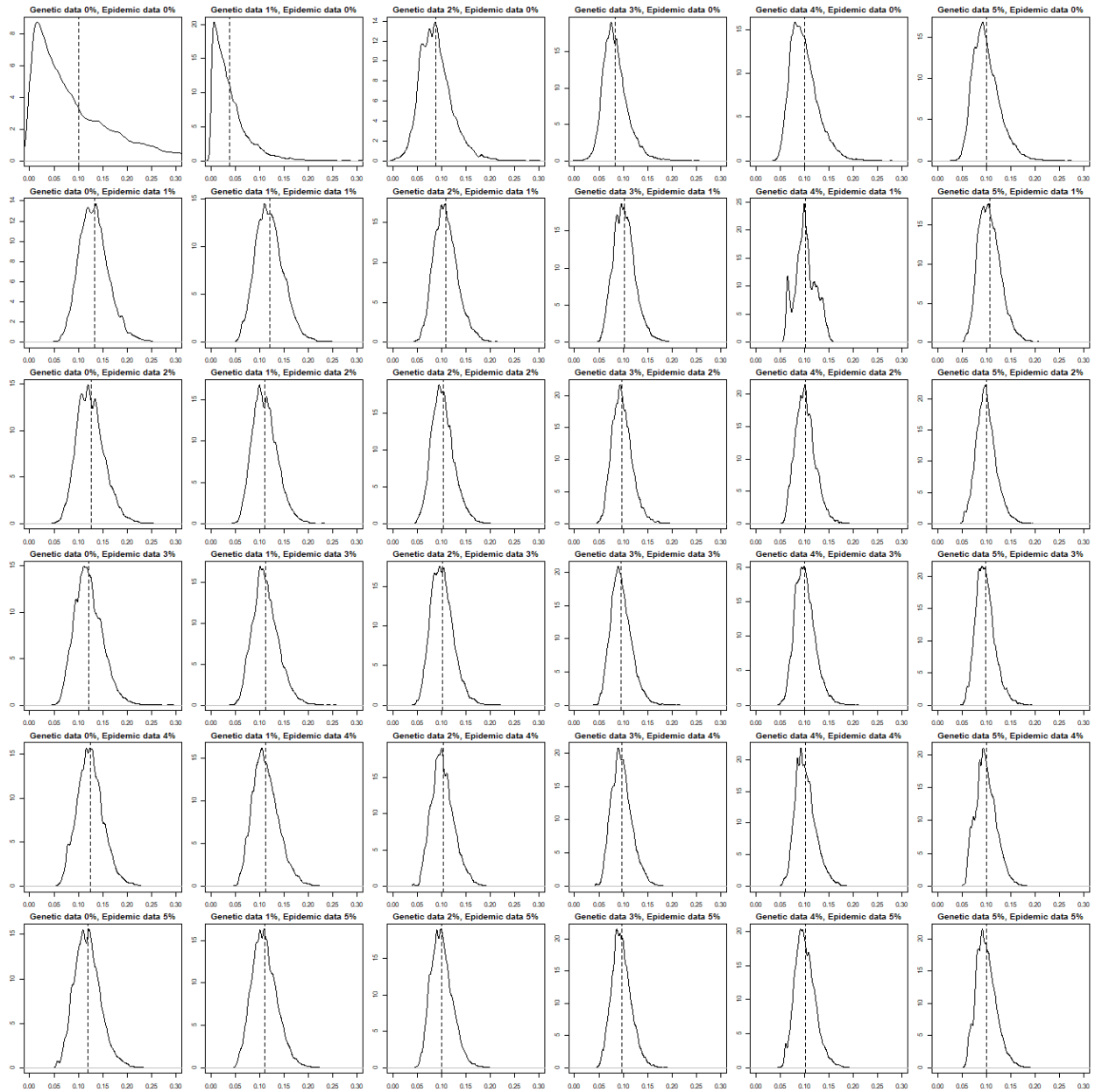


Figure 33: Posterior density of σ for a simulated epidemic with a change point birth rate. The dashed black line represents the posterior mean.

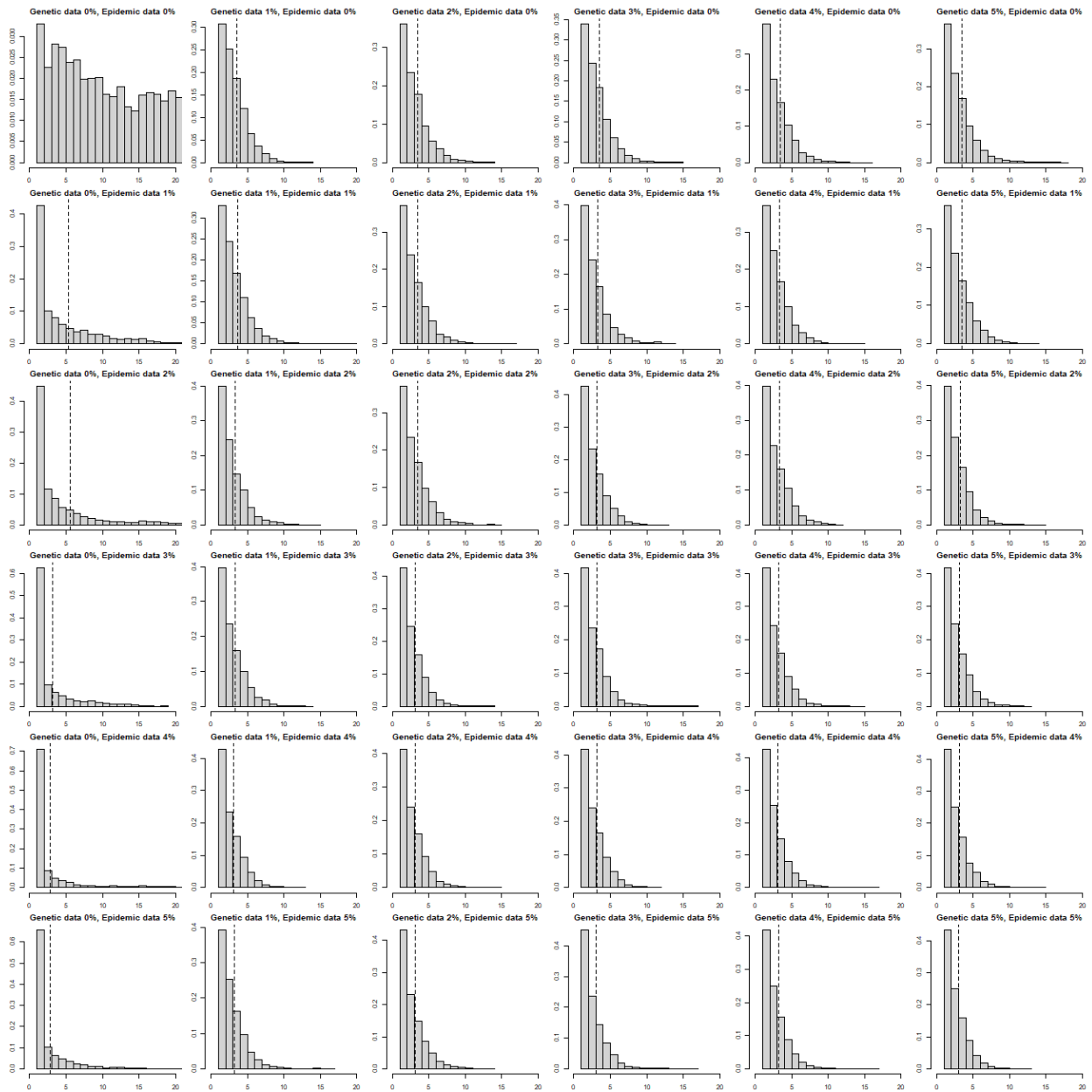


Figure 34: Posterior density histogram of the number of cases on day 0 for a simulated epidemic with a change point birth rate. The dashed black line represents the posterior mean.

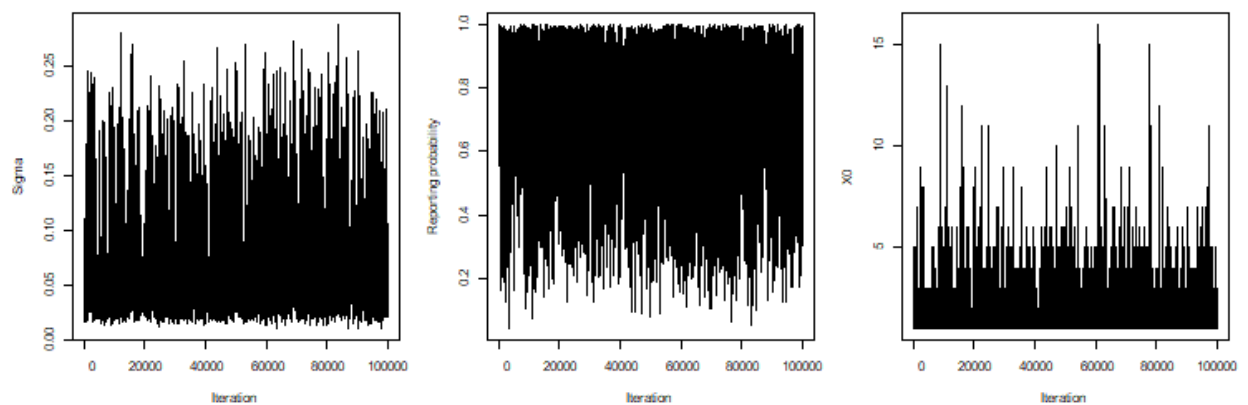


Figure 35: Trace plots for σ , ρ and X_0 for the HIV-1 data set.